Proposal for J-PARC 30 GeV Proton Synchrotron

Gamma-Ray Spectroscopy of Light Λ Hypernuclei II

Y. Akazawa, M. Fujita, N. Ichige, M. Ikeda, T. Koike, K. Miwa, Y. Ogura,
H. Tamura(spokesperson), Y. Sasaki, S. Suto, T. Yamamoto
Department of Physics, Tohoku University, Japan

K. Aoki, T. Takahashi, M. Ukai
Institute of Particle and Nuclear Studies, High Energy Accelerator Research Organization (KEK), Japan

K. Hosomi, K. Tanida
Advanced Science Research Center, Japan Atomic Energy Agency (JAEA), Japan

P. Evtoukhovitch, Z. Tsamalaidze
Joint Institute for Nuclear Research, Russia

S. Yang
Department of Physics and Astronomy, Seoul National University, Korea

R. Honda
Department of Physics, Osaka University, Japan

K. Shirotori
Research Cetner for Nuclear Physics, Osaka University, Japan

E. Botta
Dipartimento di Fisica, Universitá di Torino, and
Istituto Nazionale di Fisica Nucleare (INFN), Sezione di Torino, Italy

A. Feliciello
Istituto Nazionale di Fisica Nucleare (INFN), Sezione di Torino, Italy

M. Agnello
Dipartimento di Scienze Applicate e Tecnologia, Politecnico di Torino, Italy

Abstract

Following our successful runs of the E13 (1st part) experiment for ${}^{4}_{\Lambda}$He and ${}^{19}_{\Lambda}$F hypernuclei performed in April and June of 2015, we propose here the following studies of ${}^{4}_{\Lambda}$H and ${}^{7}_{\Lambda}$Li hypernuclei via precision γ-ray spectroscopy technique.

(1) We will measure the ${}^{4}_{\Lambda}$H$(1^+ \to 0^+)$ γ transition energy with Ge detectors to definitely confirm a large charge symmetry breaking effect in $A = 4$ hypernuclei, which was found in our previous experiment J-PARC E13 by observing the ${}^{4}_{\Lambda}$He$(1^+ \to 0^+)$ γ transition, and to provide reliable and precise data to theorists.

(2) We will precisely measure the g-factor of Λ hyperon in a nucleus via γ-ray spectroscopy of ${}^{7}_{\Lambda}$Li hypernuclei. It will be the first measurement of the baryon's g-factor inside a nucleus. It may reveal a possible modification of a baryon in nuclear matter due to a possible effect of partial restoration of chiral symmetry and/or baryon-baryon mixing in nuclear matter.

Employing the K1.1 beam line and the SKS spectrometer system, we produce excited states of these hypernuclei using 0.9 GeV/c and/or 1.1 GeV/c (K^-, π^-) reaction. We detect γ rays from hypernuclei using Hyperball-J, a large germanium detector array developed for hypernuclear γ-ray spectroscopy at J-PARC and successfully employed in E13.

(1) For the ${}^{4}_{\Lambda}$H study, the ${}^{4}_{\Lambda}$H(1^+) state is produced by ^{7}Li(K^-,π^-) reaction as a hyperfragment via highly excited unbound ${}^{7}_{\Lambda}$Li* states, and the $1^+ \to 0^+$ γ-ray energy will be determined in a 5 keV accuracy. We request 6 days for the ${}^{4}_{\Lambda}$H run.

(2) We will measure the reduced transition probabilities ($B(M1)$) of the Λ spin-flip $M1$ transitions and extract the g-factor of Λ inside a nucleus. For this purpose, we measure the ${}^{7}_{\Lambda}$Li$(3/2^+ \to 1/2^+)$ lifetime, where the $3/2^+$ state is populated from the $1/2^+(T = 1)$ state via the fast $1/2^+(T = 1) \to 3/2^+$ transition as well as from the spin-flip direct production of the $3/2^+$ state. A Li_2O target is used to optimize the stopping time in the target for Doppler shift attenuation method. In order to measure the $B(M1)$ value in an accuracy of 6%, (which corresponds to the accuracy of 3% in $|g_\Lambda - g_c|$), about 2000 events of $3/2^+ \to 1/2^+$ γ ray is necessary. We request 35 days for physics run.

In both experiments, we assume beam intensities of 1.8×10^5 K^- beam per spill for $p_{K^-} =$ 1.1 GeV/c and 0.56×10^5 K^- beam per spill for $p_{K^-} = 0.9$ GeV/c, that are expected for 50 kW and 6 s cycle operation of the acclelrator.

Before the physics run, we study the sensitivity for $B(M1)$ measurement by taking test data at 1.1 and 0.9 GeV/c K^- momenta for 2 days each. In addition, we request 10 days for a detector commissioning and beam tuning at 1.1 and 0.9 GeV/c, and 5 days for various control runs.

The experimental setup is essentailly the same as the previous experiment E13 which we successfully carried out at the K1.8 beam line in 2015. The SKS magnet is now being moved to the K1.1 area from K1.8, while the downstream part of the K1.1 beam line has to be prepared. Almost all the detectors for the K1.1/SKS spectrometers and Hyperball-J are ready. We hope to run this experiment after the E03 experiment at K1.8 probably in 2017.

1 Purpose and background

1.1 Experiment (1): Motivation –Charge Symmetry Breaking (CSB)

Charge symmetry breaking (CSB) in strong interaction is originated from mass difference between up and down quarks, but quantitative explanation of CSB phenomena in hadrons and nuclei requires microscopic understanding of hadron structure and hadron-hadron interactions together with their many-body effects.

The CSB in ΛN interaction is a hot topic in strangeness nuclear physics now. It has been suggested by old emulsion experiments [1] that the Λ binding energy of the ${}^{4}_{\Lambda}\mathrm{He}(0^+)$ ground state and that of the mirror hypernucleus ${}^{4}_{\Lambda}\mathrm{H}(0^+)$ is different by 350 ± 60 keV as shown in Fig. 1. This difference is much larger than the ${}^{3}\mathrm{He}$ and ${}^{3}\mathrm{H}$ mass difference of about 60 keV (when Coulomb effect is removed), and cannot be explained by few-body calculations based on any realistic hyperon-nucleon interaction models [2]. Recently, the Λ binding energy B_Λ for ${}^{4}_{\Lambda}\mathrm{H}(0^+)$ measured via an independent method using ${}^{4}_{\Lambda}\mathrm{H} \rightarrow {}^{4}\mathrm{He}\ \pi^-$ weak decay confirmed the emulsion value [3].

In April 2015, we carried out the J-PARC E13 experiment (the 1st part of the "E13 revised run plan") and successfully observed a γ transition for ${}^{4}_{\Lambda}\mathrm{He}(1^+ \rightarrow 0^+)$ (see Fig. 2) at $1.406 \pm 0.002 \pm 0.002$ MeV using germanium (Ge) detectors [4]. It is surprisingly large compared to the energy (1.09 ± 0.02 MeV) of the same transition for the mirror hypernucleus, ${}^{4}_{\Lambda}\mathrm{H}(1^+ \rightarrow 0^+)$,

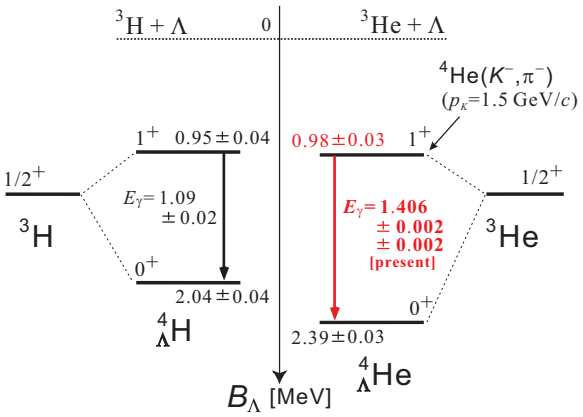

Figure 1: Level schemes of the mirror hypernuclei, ${}^{4}_{\Lambda}\mathrm{H}$ and ${}^{4}_{\Lambda}\mathrm{He}$. A large charge symmetry breaking in the ΛN interaction was confirmed from the ${}^{4}_{\Lambda}\mathrm{He}(1^+ \rightarrow 0^+)$ γ ray (shown in red). [4].

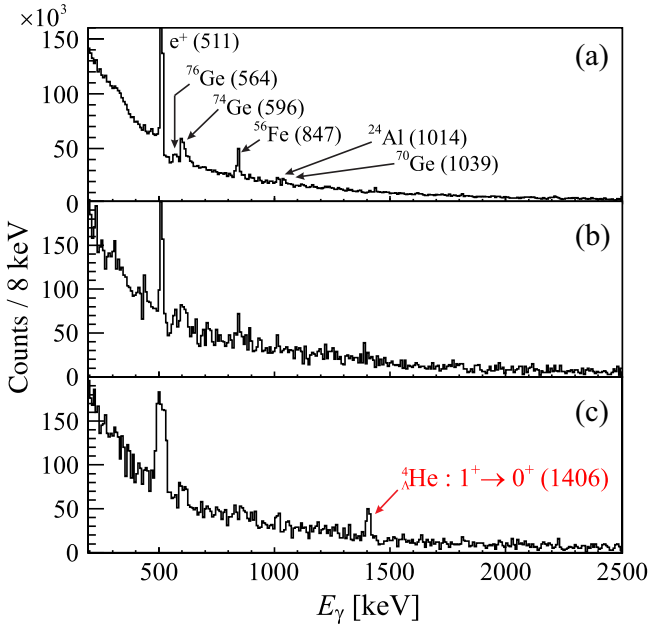

Figure 2: γ-ray spectrum for ${}^{4}_{\Lambda}\mathrm{He}$ measured in the E13 experiment via ${}^{4}\mathrm{He}(K^-,\pi^-)$ reaction [4]. (a): a highly unbound mass region is selected; (b): ${}^{4}_{\Lambda}\mathrm{He}$ bound mass region is selected; (c): the same as (b) but with event-by-event Doppler shift correction applied.

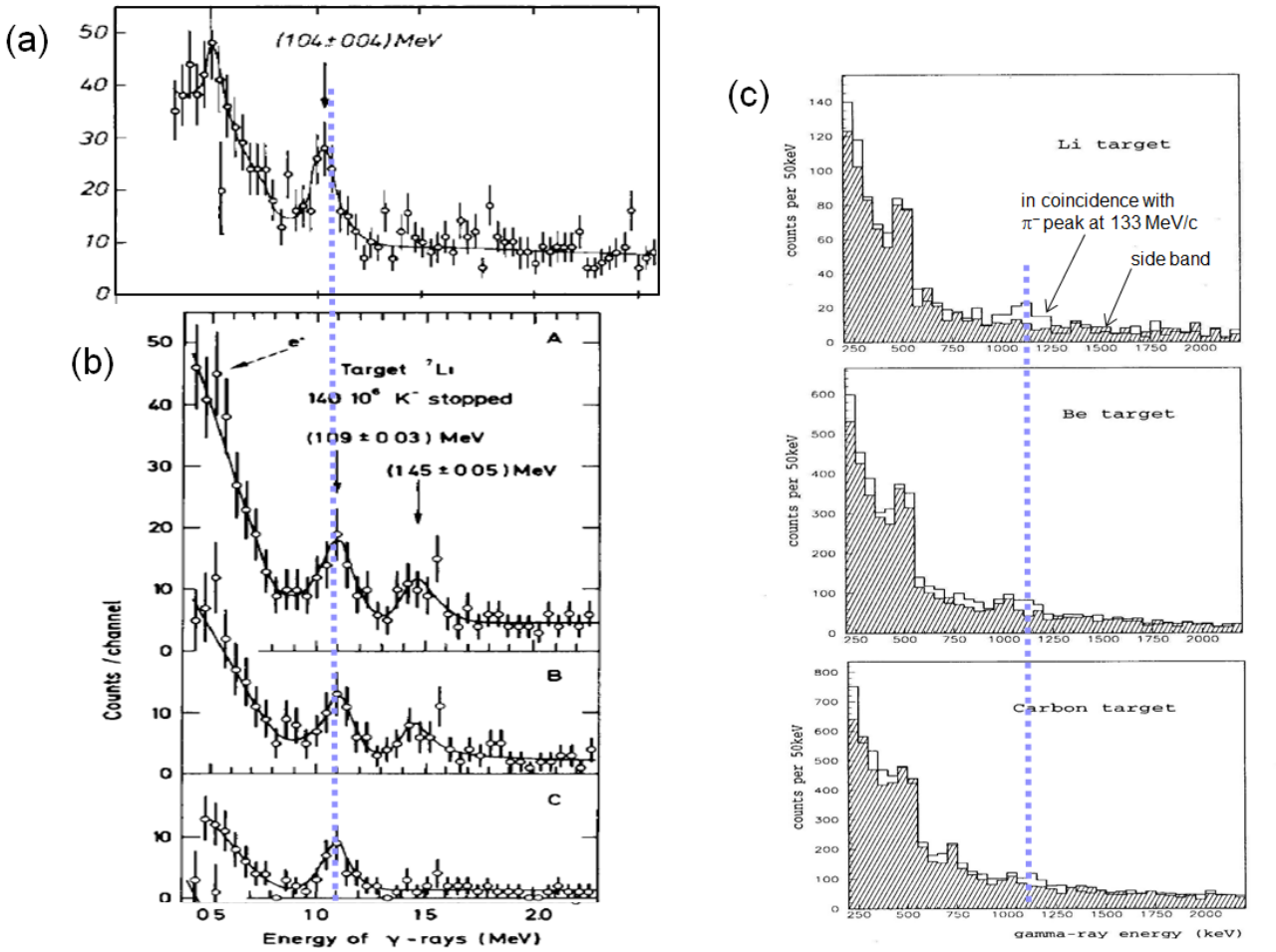

Figure 3: γ-ray spectra for ${}^{4}_{\Lambda}$H measured in old experiments, (a): stopped K^- on ^{6}Li and ^{7}Li in coincidence with 48–58 MeV charged pions.[5]; (b): stopped K^- on ^{7}Li in coincidence with charged particles [6] (in coincidence with one or two particles (A), with one particle (B), and with one 46–58 MeV charged pion (C)); (c): stopped K^- on ^{nat}Li, ^{9}Be and ^{12}C targets in coincidence with 50–57 MeV π^- [7].

as shown in the level schemes in Fig. 1. This result clearly indicated the existence of charge symmetry breaking in ΛN interaction [4].

The observed energy difference between the ${}^{4}_{\Lambda}$H$(1^+,0^+)$ splitting and the ${}^{4}_{\Lambda}$He$(1^+,0^+)$ splitting is much larger than few-body calculation results based on several realistic ΛN interaction models [2]. When combined with the $B_\Lambda(0^+)$ values (suggested to be $B_\Lambda[{}^{4}_{\Lambda}\mathrm{He}(0^+)] - B_\Lambda[{}^{4}_{\Lambda}\mathrm{H}(0^+)] = 350 \pm 60$ keV from the emulsion data only and 270 ± 95 keV with the ${}^{4}_{\Lambda}$H weak decay data), our γ-ray result suggests a very small $B_\Lambda[{}^{4}_{\Lambda}\mathrm{He}(1^+)] - B_\Lambda[{}^{4}_{\Lambda}\mathrm{H}(1^+)]$ value, implying spin dependence of the ΛN CSB interaction.

Motivated by these experimental data, theoretical efforts have recently restarted to explain the observed CSB effect (for example, see Ref. [8, 9]), that can be a touchstone for our understanding of microscopic hyperon-nucleon interactions and their many-body effects. To discuss

CSB effects in detail, precise and reliable data with accuracy of the order of 10 keV is desirable. In addition, since high precision ab-initio calculations are available for few-body hypernuclear systems (for example, see Refs. [2, 10, 11, 9]), precise data of light hypernuclear systems are of great importance.

In contrast to our ${}^{4}_{\Lambda}\mathrm{He}({}^{+}1to0^{+})$ γ-ray data, quality of ${}^{4}_{\Lambda}\mathrm{H}({}^{+}1to0^{+})$ γ-ray data is not satisfactory. It is known that among light ($A \leq 6$) hypernuclei only ${}^{4}_{\Lambda}\mathrm{H}$ and ${}^{4}_{\Lambda}\mathrm{He}$ have bound excited states. Thus the ${}^{4}_{\Lambda}\mathrm{H}$ and ${}^{4}_{\Lambda}\mathrm{He}$ γ rays were studied by producing them as hyperfragments using ${}^{7}\mathrm{Li}$ (or ${}^{6}\mathrm{Li}$) targets. The ${}^{4}_{\Lambda}\mathrm{H}(1^{+} \rightarrow 0^{+})$ transition energy of 1.09 ± 0.02 MeV in Fig. 1 is the world average of the values reported by old three hyperfragment experiments (see Fig. 3), 1.04±0.04 MeV [5], 1.09±0.03 MeV[6], 1.114±0.015±0.015 MeV [7]. The three values are sacttered although they are not inconsistent with each other. All of these experiments employed NaI counters having much worse resolution ($\sim$ 0.1 MeV (FWHM) at 1 MeV) than Ge detectors ($\sim$2 keV (FWHM) at 1 MeV). They used stopped K^{-} absorption reaction on ${}^{7}\mathrm{Li}$ and other nuclei in coincidence with charged pions from ${}^{4}_{\Lambda}\mathrm{H} \rightarrow {}^{4}\mathrm{He} + \pi^{-}$ weak decay ($E_{\pi^{-}} = 53$ MeV). Such hyperfragment production from stopped K^{-} suffers from a large and uncorrectable Doppler broadening ($\sim \pm 0.05$ MeV). The peak center of those broad peaks may be affected by a background shape (or possible background γ-ray lines) under the ${}^{4}_{\Lambda}\mathrm{H}$ peak as well as possible larger gain shift of NaI counters than Ge detectors. In addition, statistical quality of those data are limited as shown in Fig. 3.

Since the existence of a large CSB effect between ${}^{4}_{\Lambda}\mathrm{H}$ and ${}^{4}_{\Lambda}\mathrm{He}$ has been reported only from the precise measurement of ${}^{4}_{\Lambda}\mathrm{He}$ γ-ray energy, precise measurement of ${}^{4}_{\Lambda}\mathrm{H}$ γ-ray energy in similar quality, using Ge detectors and with controlled Doppler shift effects, is also desired. One of our proposing experiment is to precisely determine the ${}^{4}_{\Lambda}\mathrm{H}$ γ-ray energy using our Ge detectors.

1.2 Experiment (2): Motivation $-B(M1)$ measurement

Using hyperons free from Pauli effect from nucleons in a nucleus, we can investigate possible modification of baryons in nuclear matter. Here we propose to investigate the magnetic moment of Λ hyperon in a nucleus.

The magnetic moments of baryons are well described by the picture of constituent quark models in which each constituent quark has a magnetic moment of a Dirac particle having a constituent quark mass. If the mass of constituent quarks is changed in a nucleus by possible partial restoration of chiral symmetry, the magnetic moment of the baryon may be changed in a nucleus. A Λ hyperon in a hypernucleus is the best probe to see whether such an effect really exists or not.

Possible change of the magnetic moment of Λ in a nucleus has attracted attention of nuclear physicists. It was first pointed out [12] that Pauli effect in the quark level, if it exists, may modify a hyperon in a hypernucleus and change its magnetic moment. Then a calculation with the quark cluster model [13] showed that the "quark exchange current" between two baryons at a short distance changes the magnetic moment, of which effect depends on the confinement size of the hyperon in the nucleus.

Beside such exotic effects, magnetic moments of Λ hypernuclei have been discussed as an important subject because they are affected by Σ admixture in Λ hypernuclei due to ΛN-ΣN mixing, as well as meson exchange current between a Λ and a nucleon. Dover *et al.*

[15] estimated the effect of ΛN-ΣN mixing and found it sizable for hypernuclei with non-zero isospin (2%–5% enhancement for ${}^{4}_{\Lambda}$He and 11%–26% suppression for ${}^{15}_{\Lambda}$C), and much smaller for zero-isospin hypernuclei.

In addition, meson exchange current is expected to be different from the NN case, because in the ΛN interaction one-pion exchange is forbidden but kaon exchange as well as pion exchange in ΛN-ΣN coupling results in additional effects. The $B(M1)$ values and the magnetic moments of several s and p-shell hypernuclei were calculated [16], and these effects were found to be of the order of several %. For example, $B(M1)$ of ${}^{7}_{\Lambda}$Li$(3/2^+ \rightarrow 1/2^+)$ was calculated to be reduced by 7%. Accurate measurement of $B(M1)$ values for several hypernuclei will reveal these effects.

Direct measurement of hypernuclear magnetic moments is extremely difficult because of its short lifetime for spin precession. Here we propose to derive the g-factor of Λ in a nucleus from a probability ($B(M1)$ value) of a spin-flip $M1$ transition between the upper and lower members of a hypernuclear spin doublet. As shown in Fig. 4, each nuclear level in an ordinary nucleus ("core nucleus" of hypernucleus) with non-zero spin splits into a doublet when a Λ hyperon is added. For the two states in this doublet, the Λ spin direction is opposite to each other with respect to the core spin, and the transition between the two members of the doublet corresponds to a flip of the Λ spin. In weak coupling limit between the Λ and the core nucleus, the $B(M1)$ value of such a transition can be expressed as [14]

$$\begin{aligned} B(M1) &= (2J_{up}+1)^{-1} \mid < \phi_{low} \| \boldsymbol{\mu} \| \phi_{up} > \mid^2 \\ &= (2J_{up}+1)^{-1} \mid < \phi_{low} \| \ g_c \mathbf{J}_c + g_\Lambda \mathbf{J}_\Lambda \ \| \phi_{up} > \mid^2 \\ &= (2J_{up}+1)^{-1} \mid < \phi_{low} \| \ g_c \mathbf{J} + (g_\Lambda - g_c) \mathbf{J}_\Lambda \ \| \phi_{up} > \mid^2 \\ &= \frac{3}{8\pi} \frac{(2J_{low}+1)}{(2J_c+1)} (g_c - g_\Lambda)^2, \end{aligned} \tag{1}$$

where g_c and g_Λ denote effective g-factors of the core nucleus and the Λ hyperon, $\mathbf{J}_c$ and $\mathbf{J}_\Lambda$ denote their spins, and $\mathbf{J} = \mathbf{J}_c + \mathbf{J}_\Lambda$ is the spin of the hypernucleus, respectively. Here the spatial components of the wave functions for the lower state and the upper state of the doublet, ϕ_{low} and ϕ_{up} (with spin J_{low} and J_{up}) can be assumed to be identical.

The reduced transition probability $B(M1)$ can be derived from the lifetime τ of the excited state as

$$1/\tau = \frac{16\pi}{9} \ E_\gamma^3 \ B(M1),$$

in which the lifetime is obtained by analyzing a partly-Doppler-broadened γ-ray peak shape when the stopping time of the recoiling excited hypernucleus in the target material is of the same order as the lifetime of the γ-emitting excited state. This method called Doppler shift attenuation method (DSAM) was successfully applied to hypernuclei in KEK E419; as shown in the right inset of Fig. 5 (a), we measured the lifetime of the ${}^{7}_{\Lambda}$Li$(5/2^+)$ state from the partly-Doppler-broadened peak shape of the $5/2^+ \rightarrow 1/2^+$ γ ray, and obtained the $B(E2)$ value of this transition. The result confirmed the hypernuclear shrinking effect [18].

From this ${}^{7}_{\Lambda}$Li spectrum the $B(M1)$ value of the spin-flip $3/2^+ \rightarrow 1/2^+$ transition was not able to be obtained, because the stopping time was too long ($\sim$12 ps) compared with the $3/2^+$-state lifetime ($\sim$ 0.5 ps) and thus the γ-ray peak was fully broadened by Doppler shift.

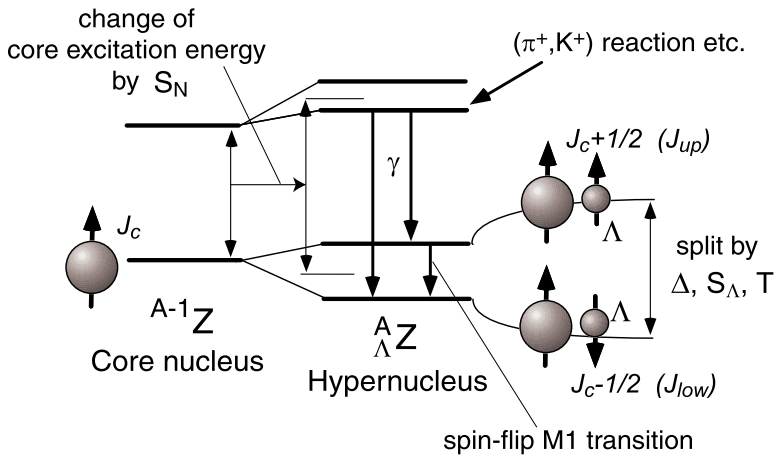

Figure 4: Spin doublet and spin-flip $M1$ transition in a hypernucleus. When a Λ is coupled to the core nucleus with spin J_c, the level is split into a doublet ($J_c + 1/2$, $J_c - 1/2$). The spin flip of the Λ gives rise to the $M1$ transition from the upper to the lower state in the doublet, and its probability $B(M1)$ is proportional to $(g_c - g_\Lambda)^2$, where g_c and g_Λ denote g-factors of the core nucleus and the Λ particle inside the nucleus (see text).

After that, measurements of Λ-spin-flip $B(M1)$ values were attempted three times in BNL E930('01) for ${}^{7}_{\Lambda}$Li, KEK E581 for ${}^{11}_{\Lambda}$B and KEK E566 for ${}^{12}_{\Lambda}$C, but accurate $B(M1)$ values were not obtained. In the E930('01) experiment, the spin-flip state of ${}^{7}_{\Lambda}\mathrm{Li}(3/2^+)$ was produced as a hyperfragment from highly excited unbound states of ${}^{10}_{\Lambda}$B by the reaction, ${}^{10}\mathrm{B}(K^-,\pi^-){}^{10}_{\Lambda}\mathrm{B}^*$, ${}^{10}_{\Lambda}\mathrm{B}^* \rightarrow {}^{7}_{\Lambda}\mathrm{Li}^* + {}^{3}\mathrm{He}$. As shown in Fig. 6, the peak shape of the ${}^{7}_{\Lambda}\mathrm{Li}(3/2^+ \rightarrow 1/2^+$, 692 keV) transition was analyzed and the lifetime of the $3/2^+$ state was derived to be $0.58^{+0.38}_{-0.20}$ ps (statistical error only), from which the $B(M1)$ was obtained as $0.30^{+0.12}_{-0.16}$ $[\mu_N^2]$ (preliminary). This value corresponds to $g_\Lambda({}^{7}_{\Lambda}\mathrm{Li}) = -1.1^{+0.6}_{-0.4}$ $[\mu_N]$, which is compared with the free-space value of $g_\Lambda = -1.226$ $[\mu_N]$. In order to measure spin-flip $B(M1)$ vslues with better accuracy, we performed KEK E518 and E566. In E518, we observed six γ rays in ${}^{11}_{\Lambda}$B [19] but complete level assignment was not possible because of low statistics which did not allow $\gamma\gamma$ coincidence method. In E566, we observed the spin-flip $M1$ transitions of ${}^{11}_{\Lambda}\mathrm{B}(7/2^+ \rightarrow 5/2^+)$ [20], but unfortunately this transition energy is found to be much lower than expected and therefore the transition is too slow to measure the lifetime by DSAM. This experiment also observed a spin-flip $M1$ transition in the ${}^{12}_{\Lambda}$C ground state doublet ($2^+ \rightarrow 1^+$) [21], but this is also too slow to apply DSAM.

In the proposing experiment, we use the ${}^{7}_{\Lambda}$Li hypernucleus to measure the spin-flip $B(M1)$ value, because the bound-state level scheme of ${}^{7}_{\Lambda}$Li is perfectly known from our γ-ray spectroscopy experiments at KEK-PS [17] and BNL-AGS [22], and thus the feasibility of the ${}^{7}_{\Lambda}$Li $B(M1)$ measurement can be most reliably estimated. Figure 7 shows the level scheme of ${}^{7}_{\Lambda}$Li, where the excitation energies measured by our previous experiments are given.

Equation 1 holds in the limit of weak coupling between a Λ and a core nucleus, in which the Λ does not change the structure of the core nucleus. It is possible, however, that the Λ may affect the structure of the core nucleus and change its magnetic moment, as the "core polarization"

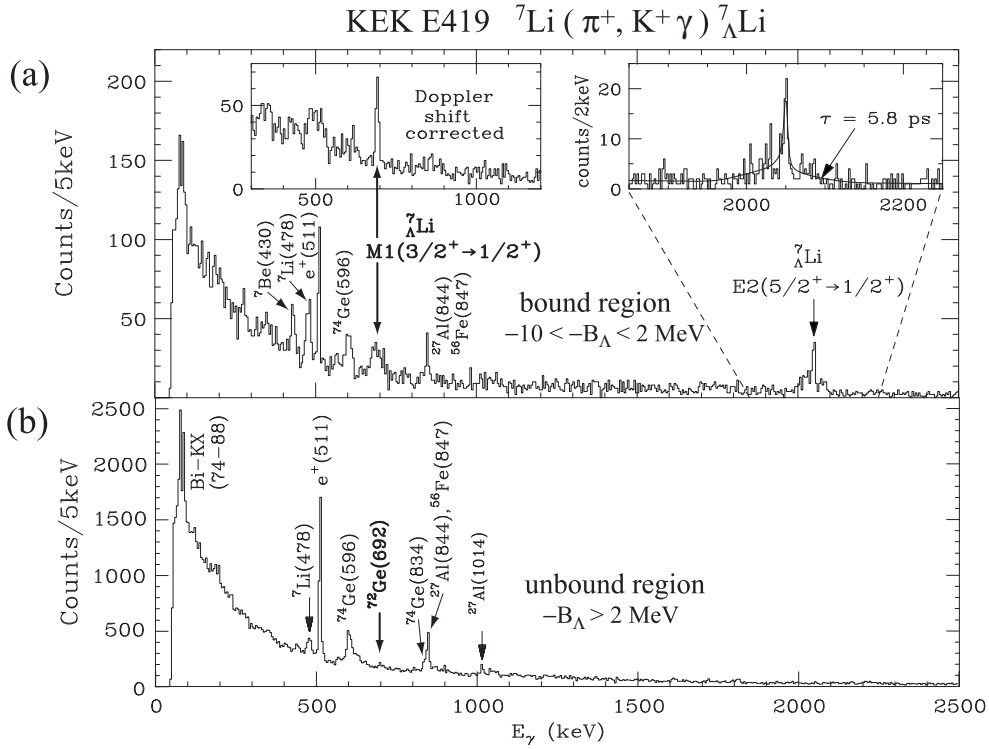

Figure 5: γ-ray spectrum of $^{7}_{\Lambda}$Li measured in KEK E419 [17]. (a) The $^{7}_{\Lambda}$Li bound state region is selected. The broad peak at 692 keV, which becomes sharp after event-by-event Doppler-shift correction (see the upper left inset), is assigned to the spin-flip $M1(3/2^+ \rightarrow 1/2^+)$ transition. The partly-broadened peak at 2050 keV is assigned to the $E2(5/2^+ \rightarrow 1/2^+)$ transition. By comparing this peak with simulated peak shapes, the lifetime of the $5/2^+$ state was obtained to be $5.8^{+0.9}_{-0.7} \pm 0.7$ ps (see the upper right inset). (b) When the unbound region of $^{7}_{\Lambda}$Li is selected, background γ rays from normal nuclei, particularly from fast-neutron induced γ rays from surrounding materials, are observed.

effect in ordinary nuclei. In hypernuclei, such effects are expected to be much smaller than in ordinary nuclei, because all the Λ-spin-dependent ΛN interaction energies (corresponding to Δ, S_Λ, and T parameters given in Sect. 1.3) have been measured to be one order of magnitude smaller than those in NN interaction from our γ-ray spectroscopy experiments; in p-shell (hyper)nuclei the ΛN spin-spin doublet splitting is typically 0.3 MeV while the NN spin-isospin doublet splitting is 3 MeV, and the ΛN spin-orbit doublet splitting is typically 0.1 MeV while the NN spin-orbit doublet splitting is 5 MeV, Therefore the "hypernuclear core polarization effects" are expected to be quite small. In fact, theoretical values of the g-factor of the $^{7}_{\Lambda}$Li ground state via shell models and cluster models predict the values close to the one from Eq. 1 (see [23], for example).

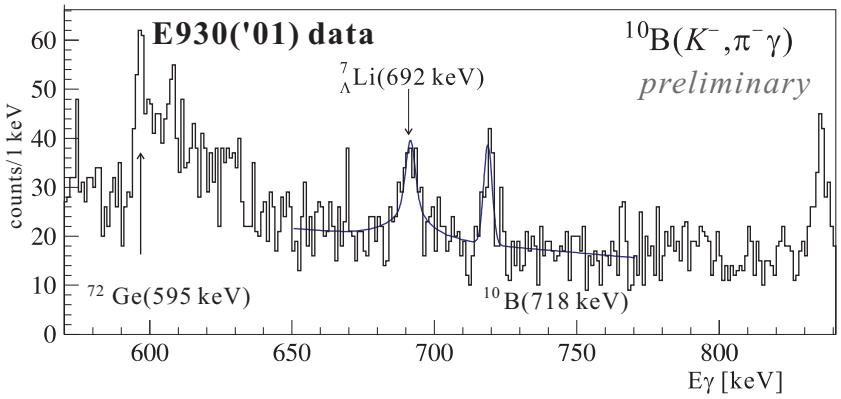

Figure 6: The γ-ray spectrum for the unbound region of $^{10}_{\Lambda}$B ($-B_\Lambda = 0-40$ MeV) in the ^{10}B $(K^-,\pi^-)^{10}_{\Lambda}$B reaction. The γ-ray peak for the $^{7}_{\Lambda}$Li$(3/2^+ \rightarrow 1/2^+)$ was observed, where the $^{7}_{\Lambda}$Li$(3/2^+)$ state is mainly produced by $^{10}_{\Lambda}$B $(s_n^{-1}s_\Lambda)\rightarrow^{7}_{\Lambda}$Li + ^{3}He. The peak shape is fitted well with a simulated peak for the $^{7}_{\Lambda}$Li$(3/2^+)$ lifetime of $0.58^{+0.38}_{-0.20}$ ps (statistical only).

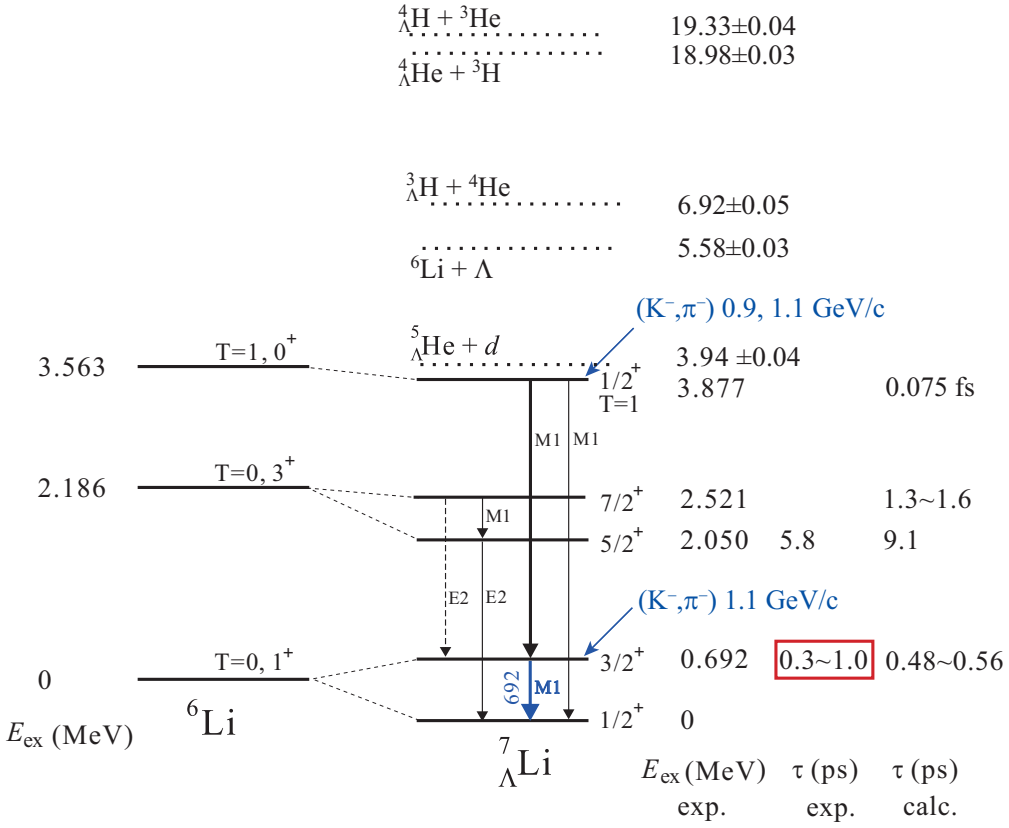

Figure 7: Level scheme of the $^{7}_{\Lambda}$Li hypernucleus. Excitation energies of all the bound states are experimentally determined [17, 22]. In the proposing experiment, we will precisely measure the lifetime of the $3/2^+$ state shown in red square from the γ-ray peak shape for the $M1(3/2^+ \rightarrow 1/2^+)$ transition shown in blue using the (K^-,π^-) reaction of $p_{K^-} = 1.1$ or 0.9 GeV/c.

1.3 Historical background and E13

Precision γ spectroscopy using germanium (Ge) detectors, which is one of the most powerful means to study nuclear structure, was introduced to hypernuclear physics at KEK-PS in 1998 by our group lead by Tohoku University. We constructed Hyperball, a large-acceptance Ge detector array equipped with fast readout electronics, and succeeded in observing hypernuclear γ rays for the first time with Ge detectors under severe backgrounds from high energy meson beams [17, 18]. The energy resolution of hypernuclear levels, which was typically a few MeV (FWHM) by magnetic spectrometers, has been drastically improved to a few keV (FWHM) by Ge detectors. Since then we have observed many γ transitions from several p-shell Λ hypernuclei, ${}^{7}_{\Lambda}$Li, ${}^{9}_{\Lambda}$Be, ${}^{11}_{\Lambda}$B, ${}^{12}_{\Lambda}$C, ${}^{15}_{\Lambda}$N and ${}^{16}_{\Lambda}$O, in KEK E419, E509, E518, E566 and BNL E930 experiments [17, 18, 24, 25, 26, 19, 22, 20, 21].

Those precise data for level structure of various p-shell hypernuclei obtained from our γ-ray spectroscopy experiments have provided us with quantitative information on the spin-dependent ΛN interaction; we determined the strengths of the ΛN spin-spin, spin-orbit, and tensor interactions as

$$\Delta = 0.33 \text{ MeV } (0.43 \text{ MeV for } A = 7),\ S_\Lambda = -0.01 \text{ MeV},\ S_N = -0.43 \text{ MeV},\ T = 0.03 \text{ MeV},$$

which correspond to the radial integrals of V_σ, V_Λ, V_N and V_T, respectively, for a nucleon in p-orbit and a Λ in s-orbit in the effective ΛN interaction:

$$V_{\Lambda N}(r) = V_0(r) + V_\sigma(r)\mathbf{s}_N\mathbf{s}_\Lambda + V_\Lambda(r)\mathbf{l}_{N\Lambda}\mathbf{s}_\Lambda + V_N(r)\mathbf{l}_{N\Lambda}\mathbf{s}_N + V_T(r)[3(\boldsymbol{\sigma}_N\hat{\mathbf{r}})(\boldsymbol{\sigma}_\Lambda\hat{\mathbf{r}}) - \boldsymbol{\sigma}_N\boldsymbol{\sigma}_\Lambda].$$

These obtained parameter values were compared with predicted values from theoretical baryon-baryon interaction models based on meson exchange picture or quark-gluon picture in order to test their validity and to improve the models.

In addition, the $B(E2)$ value in ${}^{7}_{\Lambda}\text{Li}(5/2^+ \to 1/2^+)$ was measured [18] with the Doppler shift attenuation method (DSAM) and confirmed the nuclear shrinking effect due to a Λ hyperon [27], where the core nucleus ^{6}Li was found to be contracted by 19$\pm$4%.

In J-PARC, we have planned to extend our previous study of p-shell hypernuclei to s-shell and sd-shell hypernuclei, as well as to approach a new subject on "baryon modification" though a spin-flip $B(M1)$ measurement. The J-PARC E13 experiment titled "Gamma-ray Spectroscopy of Light Hypernuclei" [28, 29] was proposed and approved in 2005. This experiment aimed at investigation of ${}^{4}_{\Lambda}$He and ${}^{19}_{\Lambda}$F levels as the 1st part, and then ${}^{7}_{\Lambda}$Li $B(M1)$ measurement and ${}^{9}_{\Lambda}$Be and ${}^{11}_{\Lambda}$B levels as the 2nd part. Considering realistic beam intensity and available beam lines, we decided to run the 1st part at the K1.8 beam line with the SKS spectrometer [30], and the 2nd part later at the K1.1 beam line after construction and movement of the K1.1 line and the SKS magnet. In April and June of 2015, the 1st part of E13 was successfully performed at K1.8 with the SKS spectrometer (SksMinus setting) and the Hypeball-J array. The ${}^{4}_{\Lambda}\text{He}(1^+ \to 0^+)$ $M1$ transition was observed at $1.406 \pm 0.002 \pm 0.002$ MeV, indicating an unexpectedly large charge symmetry breaking effect in ΛN interaction [4]. Data analysis is still ongoing for the ${}^{19}_{\Lambda}$F data, where at least two γ transitions of ${}^{19}_{\Lambda}$F have been observed.

In the last PAC meeting we were requested to resubmit a proposal for the E13 2nd part which is to be performed at the newly-constructed K1.1 beam line. Thus, here we submit a proposal corresponding to the E13 2nd part. This proposal is, however, focused on a ${}^{7}_{\Lambda}$Li

$B(M1)$ measurement, together with a short run for ${}^{4}_{\Lambda}$H study which has aroused interest due to our ${}^{4}_{\Lambda}$He result. Experiments for other subjects on hypernuclear γ-ray spectroscopy such as ${}^{10}_{\Lambda}$B and ${}^{11}_{\Lambda}$B written in the original E13 proposal, as well as possible other light hypernuclei, will be proposed later as independent proposals.

2 Experimental method

Both experiments will be carried out at the K1.1 beam line using the (K^-,π^-) reaction at p_{K^-} = 1.1 or 0.9 GeV/c, employing the SKS spectrometer and the Ge detector array, Hyperball-J.

2.1 Experiment (1): ${}^{4}_{\Lambda}$H

In order to produce the ${}^{4}_{\Lambda}$H(1^+) state, we use the in-flight ^{7}Li(K^-,π^-) reaction at p_{K^-}= 0.9 GeV/c. In an old experiment at BNL-AGS [31], ${}^{4}_{\Lambda}$H γ ray was abundantly observed by in-flight ^{7}Li(K^-,π^-) reaction at p_{K^-}= 0.82 GeV/c. Figure 8 shows a γ-ray spectrum measured in coincidence with the ^{7}Li(K^-,π^-) reaction employing NaI counters in the BNL experiment. They observed ${}^{7}_{\Lambda}$Li $E2(5/2^+ \rightarrow 1/2^+)$ transition at 2.0 MeV when the ${}^{7}_{\Lambda}$Li bound mass region is selected. In addition, they observed a peak at 1.1 MeV when selecting the highly unbound mass region of $E_{ex} = 22 - 39$ MeV ($-B_\Lambda$ = 16.4–33.4 MeV) which is above the ${}^{7}_{\Lambda}$Li$\rightarrow{}^{4}_{\Lambda}$H+^{3}He threshold ($E_{ex}$ = 19.3 MeV) shown in Fig. 7. In Ref. [31], they assigned this 1.1 MeV peak as a mixture of ${}^{4}_{\Lambda}$H and ${}^{4}_{\Lambda}$He γ rays, because the ${}^{4}_{\Lambda}$He γ-ray energy was believed to be 1.15 MeV [5] and the ${}^{4}_{\Lambda}$H γ ray to be 1.06–1.09 MeV at that time. Since we know that the ${}^{4}_{\Lambda}$He γ-ray energy is 1.406 MeV, the 1.1 MeV peak should be now ascribed only to the ${}^{4}_{\Lambda}$H($1^+ \rightarrow 0^+$) transition. This peak energy was reported to be 1.108 ± 0.010 MeV, but it may also be affected by possible background and by inhomogeneous Doppler shift inherent in in-flight (K^-,π^-) reaction method.

At p_K = 0.9 GeV/c, the $K^-n \rightarrow \Lambda\pi^-$ elementary cross section with spin-non-flip Λ production is quite large, but the spin-flip cross section is small (see Fig. 9). It is expected, however, in the ${}^{4}_{\Lambda}$H production from a ^{7}Li nucleus the spin-non-flip reaction also contributes to ${}^{4}_{\Lambda}$H(1^+) production, as suggested in stopped K^- absorption (spin-non-flip reaction) experiment on ^{7}Li target [7]. The large yield of ${}^{4}_{\Lambda}$H γ ray observed in the BNL experiment [31] at p_{K^-} = 0.82 GeV/c is thus explained. In the proposing experiment, we use a similar condition as the BNL experiment but measure the γ-ray more precisely with Ge detectors.

Although the momentum transfer in the (K^-,π^-) reaction at 0.9 GeV/c is rather small (70–160 MeV/c for 0°–10°), the γ-ray peak is significantly broadened by Doppler shift ($\sim$ 37 keV in rms) due to the break-up process in fragment production (${}^{7}_{\Lambda}$Li$^* \rightarrow {}^{4}_{\Lambda}$H* + ^{3}He) as shown in Fig. 10 (a). The red line in Fig. 10 shows an expected peak shape after Doppler shift correction for a recoiling ${}^{7}_{\Lambda}$Li* velocity by using the recoil velocity vector measured for each event from K^- and π^- momenta. The peak shape does not change, because the recoil velocity given by the fragmentation is much larger than the ${}^{7}_{\Lambda}$Li* velocity. Therefore, Doppler broadening due to the fragmentation cannot be corrected for. However, the Doppler broadening is suppressed when ${}^{7}_{\Lambda}$Li* events close to the ${}^{4}_{\Lambda}$H* + ^{3}He decay threshold (E_{ex} = 20.4 MeV) having a small recoil energy in fragmentation are selected in the missing mass spectrum. As shown in Fig. 10 (b), the peak width is narrower ($\sim$ 18 keV in rms) when the mass region of E_{ex} = 20–25 MeV

is selected.

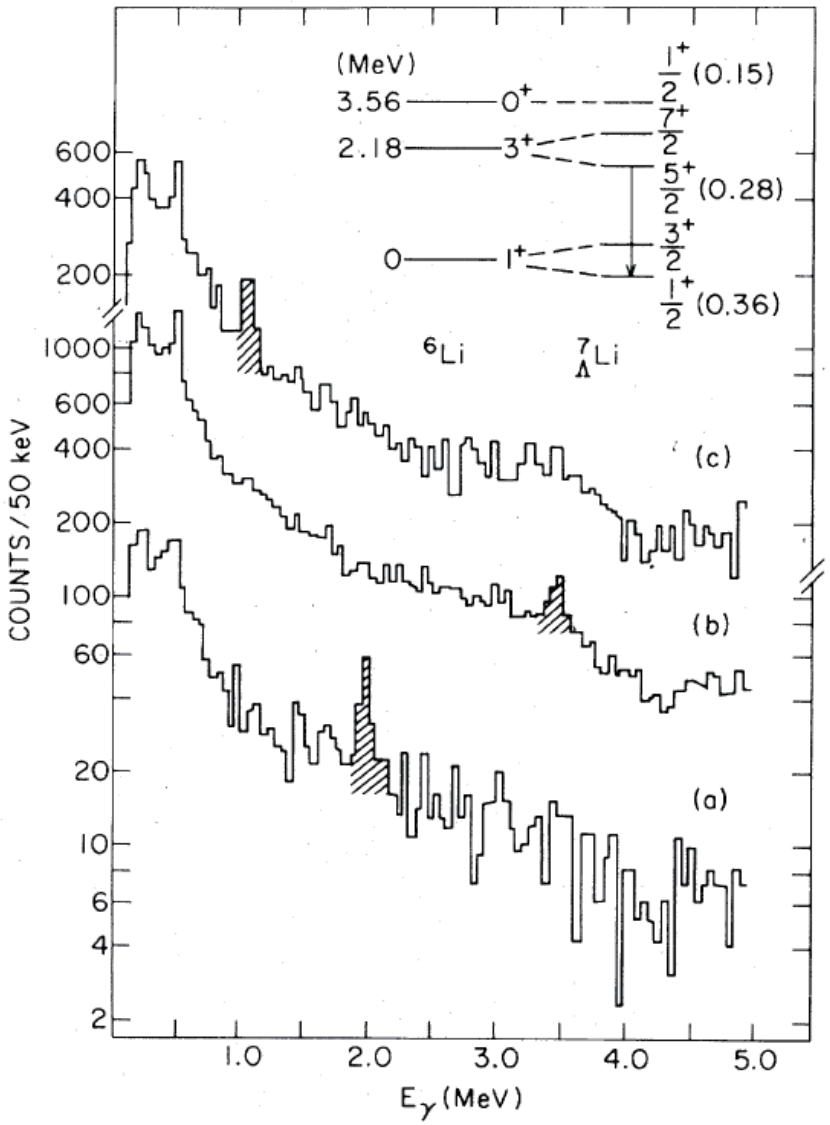

Figure 8: γ-ray spectra taken in coincidence with the in-flight ^{7}Li(K^-,π^-) reaction at p_{K^-} = 0.83 GeV/c [31]. (a) is the spectrum when the bound region of $^7_\Lambda$Li mass is selected, where the $^7_\Lambda$Li $E2(5/2^+ \rightarrow 1/2^+)$ transition is observed at 2.0 MeV. (c) is the spectrum when the unbound region of E_{ex} = 22–39 MeV in the $^7_\Lambda$Li mass is selected. A peak at 1.1 MeV is now ascribed to the $^4_\Lambda$H$(1^+ \rightarrow 0^+)$ γ ray (see text).

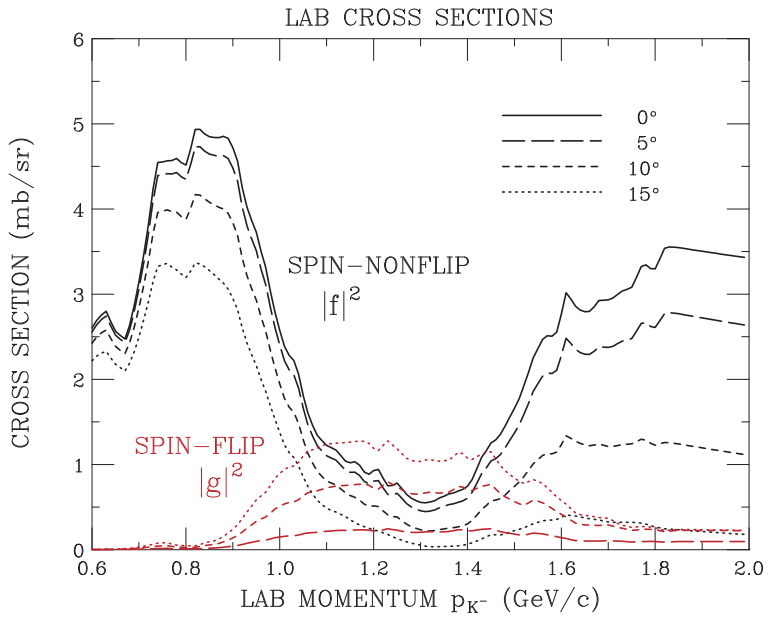

Figure 9: Non-spin-flip and spin-flip cross sections of the $K^- n \to \Lambda\pi^-$ reaction as a function of K^- momentum [32, 33].

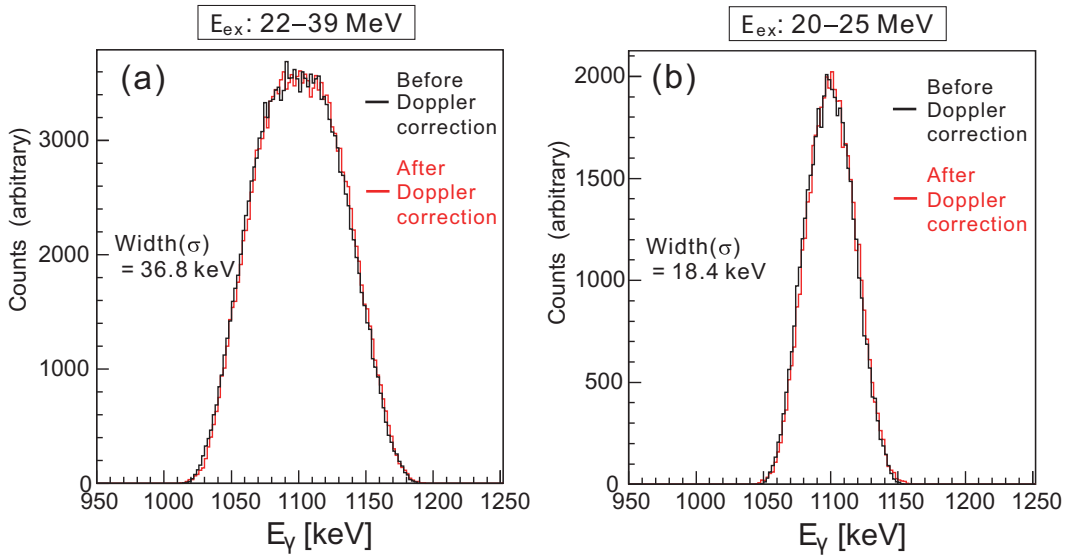

Figure 10: Simulated spectrum shape of the ${}^{4}_{\Lambda}\mathrm{H}$ γ ray peak in the ${}^{7}\mathrm{Li}(K^-,\pi^-)$ reaction at $p_{K^-} = 0.9$ GeV/c for different missing mass gates (E_{ex} is the excitation energy for ${}^{7}_{\Lambda}\mathrm{Li}$). Black and red lines show the spectra before and after Doppler shift correction for ${}^{7}_{\Lambda}\mathrm{Li}^*$.

2.2 Experiment (2)

2.2.1 Reaction

In the ${}^{7}_{\Lambda}$Li ground-state doublet ($3/2^+$,$1/2^+$), the $3/2^+$ state is produced by the spin-flip amplitude of the elementary process ($K^- + n \rightarrow \Lambda + \pi^-$), while the $1/2^+$ state (ground state) is produced by the non-spin-flip reaction. As shown in Fig. 9, the elementary cross section for the spin-flip Λ production is large for $p_{K^-} = 1.1$–1.4 GeV/c. Therefore, we choose the K^- momentum at 1.1 GeV/c, which is the maximum momentum of the K1.1 beam line giving the highest beam intensity. Since the spin-flip cross section is large at larger angles ($> 10^o$) in contrast to the non-spin-flip cross section which is large at small angles, the γ-ray background coming from non-spin-flip ${}^{7}_{\Lambda}$Li states such as the $1/2^+$ (ground state) and $5/2^+$ states is expected to be suppressed when large angles are selected. However, this selection makes the ${}^{7}_{\Lambda}$Li recoil velocity faster, which may reduce the sensitivity in DSAM.

On the other hand, the spin-flip $3/2^+$ state is also produced via the non-spin-flip $1/2^+(T{=}1)$ state at 3.88 MeV though the fast γ decay $1/2^+(T{=}1) \rightarrow 3/2^+$. The $1/2^+(T{=}1)$ state is populated by non-spin-flip reaction (see Fig. 7) with a large cross section at $p_{K^-} = 0.7$–0.9 GeV/c (see Fig. 9). In our first γ-ray spectroscopy experiment (KEK E419) [17], the yield of the ${}^{7}_{\Lambda}\mathrm{Li}(3/2^+ \rightarrow 1/2^+)$ transition was three times larger than that expected only form the direct $3/2^+$ production, and the contribution from the $1/2^+(T{=}1) \rightarrow 3/2^+$ cascade was found to be important. Therefore, the use of 0.9 GeV/c beam may be another choice, although the beam intensity is lower than at 1.1 GeV/c and the γ-ray background level is expected to be higher. As described in Sect. 4.2, our simulation (Fig. 20) shows that the sensitivity of DSAM is similar between 1.1 GeV/c beam and 0.9 GeV/c beam. Therefore, we will take test data for both beam momenta before the physics run, since the beam intensity, the production cross sections of the $3/2^+$ and $1/2^+(T = 1)$ states and the background level are not perfectly known for these momenta.

2.2.2 Lifetime and Target

Without any anomalous effect in g_Λ, the $B(M1)$ value of this transition is estimated to be $B(M1) = 0.326$ $[\mu_N^2]$ from Eq. 1 and calculated to be $B(M1) = 0.322$ $[\mu_N^2]$ from a cluster model [23], which correspond to 0.5 ps of the $3/2^+$ state lifetime.

In order to measure the lifetime by DSAM, matching between the lifetime and the stopping time of the recoiling nucleus is important. According to our simulation, the lifetime can be most accurately determined when the stopping time is 2–3 times longer than the lifetime. In our experiment, we need a high density (2–3 g/cm^3) material containing a large fraction of lithium nuclei but without other nuclei emitting many γ rays and also without other nuclei which may produce unknown hypernuclear γ rays.

Lithium oxide (Li_2O) with a density of 2.01 g/cm^3 in granular powder is the best target material for our purpose. The stopping time of the recoiling ${}^{7}_{\Lambda}$Li hypernuclei in this material is calculated to be 2–3 ps, being of the same order of the expected $3/2^+$ state lifetime around 0.5 ps and close to the ideal matching condition. We know all hypernuclear γ rays produced from ^{16}O nuclei by the (K^-,π^-) reaction (p_{K^-} =0.9 GeV/c) from our previous experiment [25, 22].

It is noted that even when the $3/2^+$ state is produced via the $1/2^+(T{=}1) \rightarrow 3/2^+$ transition,

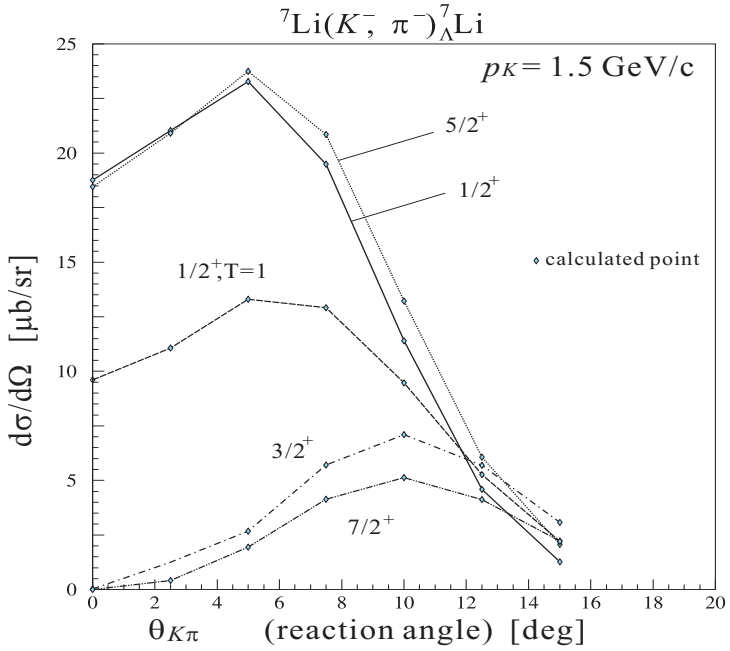

Figure 11: Cross sections of all the bound states of the $^{7}_{\Lambda}$Li hypernucleus in the (K^-,π^-) reaction at $p_{K^-} = 1.5$ GeV/c calculated by Motoba [34].

this transition is fast (theoretically estimated to be 0.075 fs [23]) and does not affect the lifetime measurement of the $3/2^+$ state.

The Li_2O target thickness is 20 g/cm^2 (10 cm thick), which is the maximum thickness we can use for hypernuclear γ-ray spectroscopy with a reasonable missing mass resolution ($\sim$6 MeV (FWHM)).

2.2.3 Background

K^- beam decay background Hypernuclear production via the (K^-,π^-) reaction suffers from background due to decays of K^- in the beam, $K^- \to \mu^-\bar{\nu}$ and $\pi^-\pi^0$. Muons and charged pions in this decay cannot be kinematically separated from π^- emitted by hypernuclear production reaction. In particular, when $K^- \to \pi^-\pi^0$ decay events are accepted in the (K^-,π^-) trigger, the Ge detectors in Hyperball-J often receive some energy deposit from electromagnetic showers of high energy photons from π^0, which causes serious background in the final γ-ray spectrum. As described in Sect. 3.4, we employ various counters for particle identification and decay background rejection. In the E13 run, those detectors enabled us to make the effect of the K^- decay background negligibly small both in the trigger level and after the off-line analysis.

Background from ^{16}O target Another serious background is caused by γ-ray and neutron emissions after reactions of a beam particle with target nuclei. In particular, a significant amount of background comes from excited nuclei via the (K^-,π^-) reaction on ^{16}O in the Li_2O target. Figure 12 is a simulated $^{7}_{\Lambda}$Li missing mass spectrum for 1.1 GeV/c (K^-,π^-) reaction on a 20 g-thick Li_2O target, where relative cross sections between $^{7}_{\Lambda}$Li and $^{16}_{\Lambda}$O states are assumed

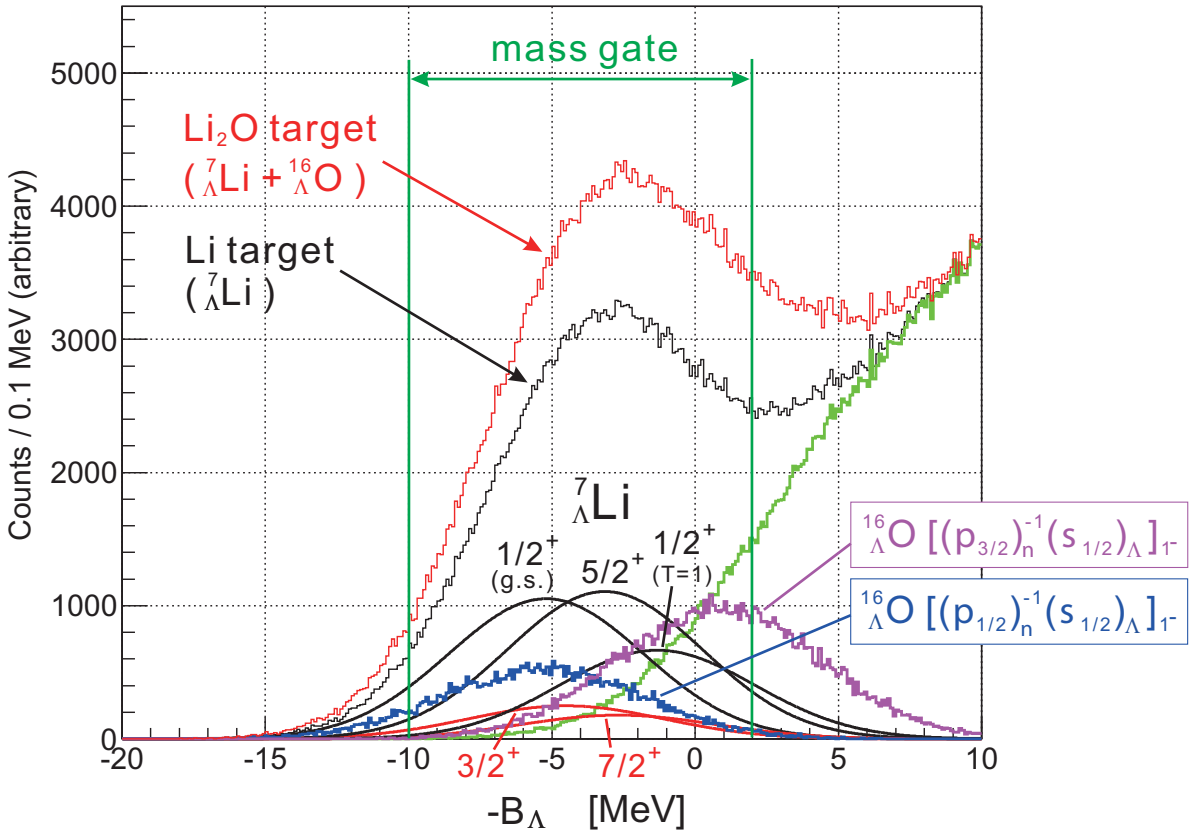

Figure 12: Expected missing mass spectrum for hypernuclei on a Li_2O target (20 g/cm^2 thick) in the (K^-,π^-) reaction at 1.1 GeV/c. Contributions of ${}^{7}_{\Lambda}$Li states (the non-spin-flip $1/2^+$, $5/2^+$ and $1/2^+(T{=}1)$ states and the spin-flip $3/2^+$ and $7/2^+$states) together with contamination from ^{16}O target nuclei for distinct two states, ${}^{16}_{\Lambda}$O(1^-) $(p_{3/2})_n^{-1}(s_{1/2})_\Lambda$) and $(p_{3/2})_n^{-1}(s_{1/2})_\Lambda$), are shown.

to be the same as the ones observed in the (π^+,K^+) reaction.

It is known that the ${}^{16}_{\Lambda}$O ground state ($(p_{1/2})_n^{-1}(s_{1/2})_\Lambda$)) and the 6 MeV excited state ($(p_{3/2})_n^{-1}(s_{1/2})_\Lambda$)) have large cross sections and they overlap with the ${}^{7}_{\Lambda}$Li bound states, as shown in Fig. 12. Those ${}^{16}_{\Lambda}$O states in the mass gate, as well as the ${}^{7}_{\Lambda}$Li$(1/2^+)$ and ${}^{7}_{\Lambda}$Li$(5/2^+)$ states contribute to the background in the mass-gated γ-ray spectrum. They increase the continuous γ-ray background level, but no γ-ray lines from ^{16}O nuclei appear around the ${}^{7}_{\Lambda}$Li$(3/2^+ \rightarrow 1/2^+)$ energy (692 keV); there are only four bound states in ${}^{16}_{\Lambda}$O and all the γ transitions from them were measured at 6–7 MeV in E930 [25], and there exist no γ-ray lines around 692 keV from ordinary nuclei with $A < 16$ that can be produced after weak decay of ${}^{16}_{\Lambda}$O and ${}^{7}_{\Lambda}$Li hypernuclei.

Several neutron-induced γ-ray lines from ordinary nuclei in the surrounding material appear in the γ-ray spectrum. Among them, the 692 keV γ ray from ^{72}Ge(n,n') can be a background for our measurement, although the lifetime of ^{72}Ge(692) γ ray is slow (641 ns) and a prompt timing cut (typically < 20 ns) almost removes this γ ray. According to our experience in E419 (see Fig. 5 (b)), a small peak from ^{72}Ge appears at 692 keV when the prompt timing cut is loose

(80 ns gate width). This background is estimated to give almost negligible effect to the ${}^{7}_{\Lambda}$Li γ-ray spectrum after a tight timing cut (20 ns gate width), and also this effect can be reliably estimated from intensities of other lines such as ^{74}Ge(596) and ^{72}Ge(834).

2.2.4 Systematic errors

In a precise determination of the lifetime of the ${}^{7}_{\Lambda}$Li($3/2^+$) state by DASM, we need to minimize systematic errors. In our $B(E2)$ measurement of ${}^{7}_{\Lambda}$Li [18] via DSAM applied to the $5/2^+ \to 1/2^+$ γ-ray peak, major systematic errors came from
(1) ambiguity of the stopping power calculation in the SRIM code,
(2) Ge detector response function, and
(3) non-uniform emission of γ rays due to alignment of hypernuclei.
In addition, we should consider a possible systematic error from
(4) effect of cascade transitions via upper states with long lifetimes.

Error (1) Measured dE/dx data for Li ion in various materials are reproduced from the calculated values in the SRIM code within $\sim$ 4% in rms [35]. We estimate that this dE/dx ambiguity causes an error of our ${}^{7}_{\Lambda}$Li stopping time of $\sim$3%.

Error (2) Possible change of the Ge response function during the experiment due to radiation damage causes a serious systematic error in DSAM. In the present case, however, such a damage effect is negligible because of our new Ge detector cooling system using pulse-tube refrigerators (see Sect. 3.5) and weaker hadron beam intensity (the total beam intensity of K^- plus π^- will be about 0.3×10^6/sill(2 s), while in the KEK E419 case π^+ beam intensity was 2.5×10^6/s with a similar distance ($\sim$ 15 cm) from the beam to the Ge detectors).

Error (3) Since the magnitude of Doppler shift has a correlation with the Ge detector position, alignment of the produced hypernuclei introduced by the $p_n^{-1} \to s_\Lambda$ ($\Delta L = 1$) reaction leads to non-uniform angular distribution of emitted γ rays and causes a deviation of the peak shape. In our case of the $3/2^+$ state, this effect is negligibly small. The cascade production of the $3/2^+$ state via the $1/2^+$ (T=1) production makes no alignment. After the direct production of the $3/2^+$ states, the $3/2^+ \to 1/2^+$ γ ray has an angular distribution which is calculated to be $\propto 1 + A\cos^2\theta$ with $A = 3/49$ [14], having a much smaller A value than the $E2(5/2^+ \to 1/2^+)$ case of $A = 3/4$.

Error (4) In the present case, we should consider a systematic error coming from a small but unknown branching ratio of the ${}^{7}_{\Lambda}$Li($5/2^+ \to 3/2^+$) transition, which is 3.4% in weak coupling limit (pure $E2$ transition) but can be changed due to $M1/E2$ mixing. Since the yield of the $5/2^+$ state is large and its lifetime is long (measured to be $5.8^{+0/9}_{-0.7} \pm 0.7$ ps [18]), the $5/2^+ \to 3/2^+$ transition affects the lifetime fit for the $3/2^+ \to 1/2^+$ transition. In the proposing experiment, we can clearly observe the $5/2^+ \to 3/2^+$ transition peak at 1358 keV and determine the branching ratio, which will be taken into account in the lifetime fit for the $3/2^+ \to 1/2^+$ transition.

Another transition, $E2(7/2^+ \rightarrow 3/2^+)$, does not cause a systematic error, because the production cross section of the spin-flip $7/2^+$ state is small and the branching ratio of $7/2^+ \rightarrow 3/2^+$ is less than 19%, as well as the lifetime of $7/2^+$ is expected to be rather short (1.3–1.6ps).

Systematic errors from other sources such as ambiguities in the reaction vertex position, the recoil direction, the recoil velocity, and so on are expected to be as small as $\sim$1% from our experience in E419.

In total, the systematic error of the lifetime determination will be 4%.

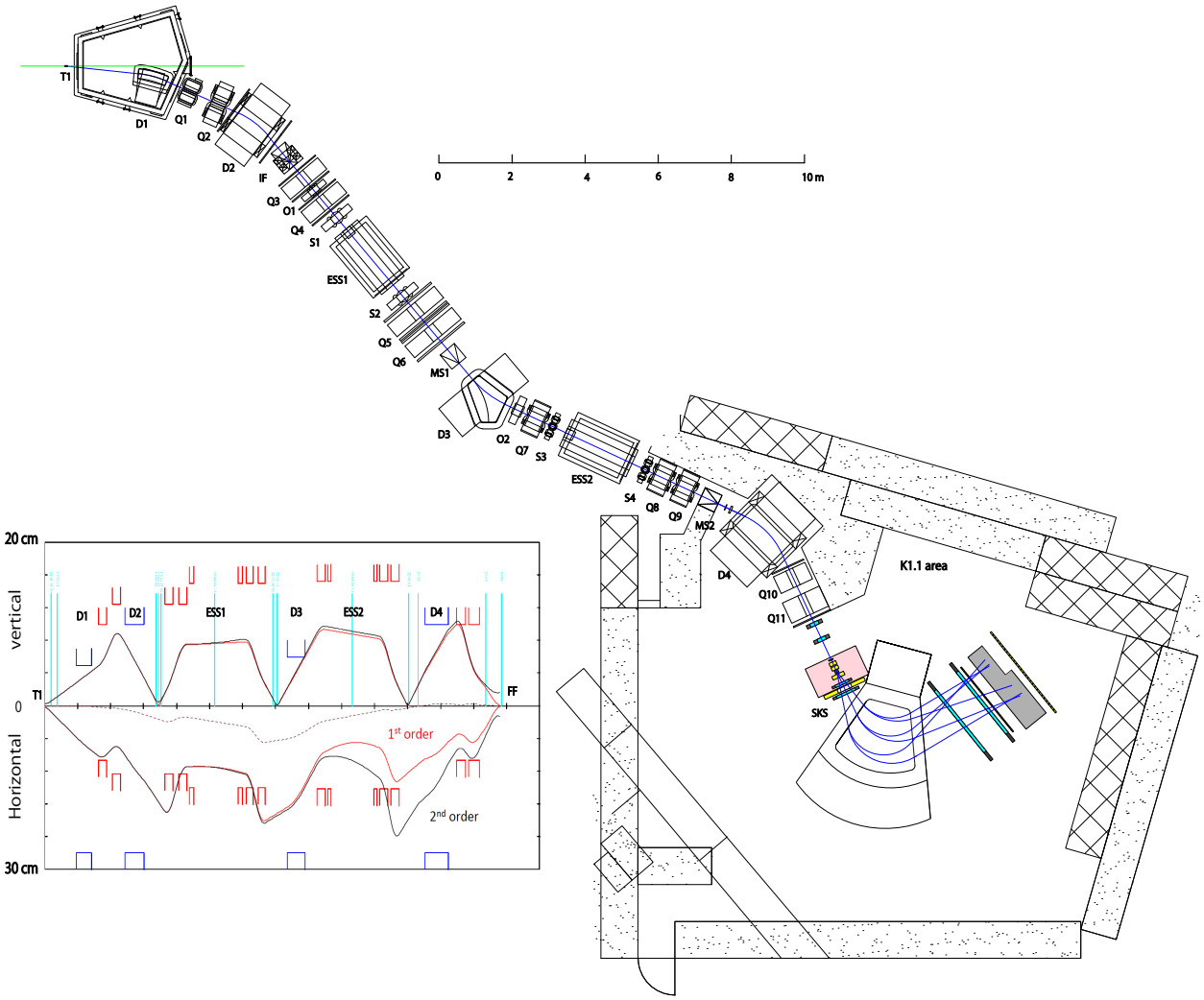

Figure 13: Layout of the K1.1 beam line and the K1.1 area. The calculated beam envelope is also shown.

3 Experimental Setup

In the proposing experiment, we employ the K1.1 beam line, the SKS spectrometer, and our Ge detector array, Hyperball-J. Figure 13 shows the K1.1 beam line and the K1.1 experimental area. The experimental setup is shown in Fig. 14. It is essentially the same as in the previous experiment E13 performed at K1.8.

3.1 K1.1 beam line

The K1.1 beam line is designed to deliver high purity kaon beams up to 1.1 GeV/c employing double-stage electrostatic separators (ESS1, ESS2) together with an intermediate focus point (IF). The layout of K1.1 and the beam envelope are shown in Fig. 13. The upstream part of

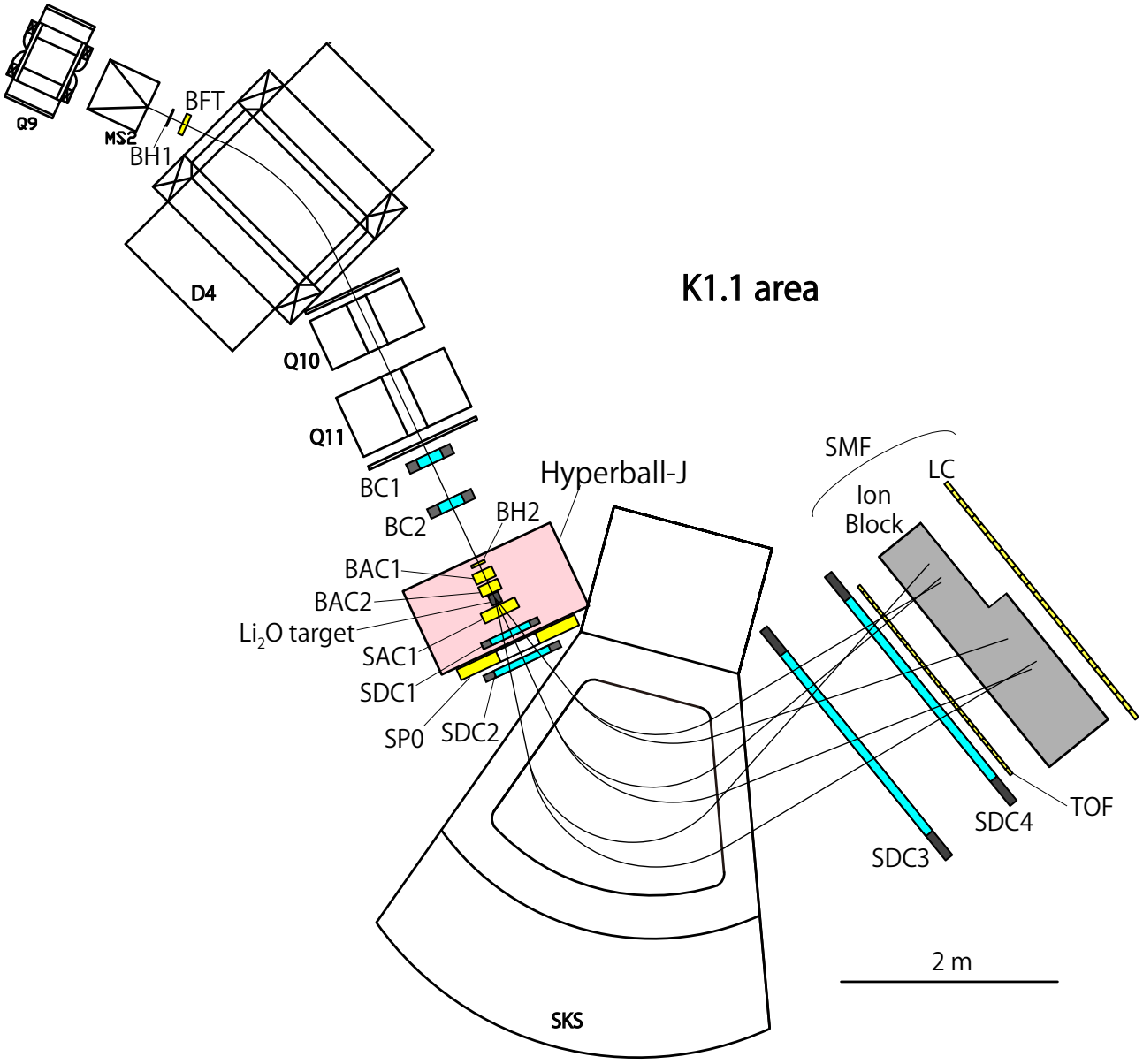

Figure 14: Experimental setup for the K1.1 beam spectrometer, the SKS spectrometer, and detectors around the target.

K1.1 has been successfully operated as the K1.1BR line. The downstream part after D3 needs to be prepared.

The K^- intensity and purity depend on the openings of the intermediate focus slit (IF) and the two mass slits (MS1, MS2). According to simulations using Decay Turtle code with various slit openings, the highest K^- intensity with a reasonably small π^- contamination was found as 1.76×10^5 K^-/spill (with a $K^-/(K^-+\pi^-)$ ratio of 0.58) for $p_{K^-} = 1.1$ GeV/c and 0.56×10^5 K^-/spill for $p_{K^-} = 0.9$ GeV/c, where the proton beam power of 50 kW and 6 s cycle operation are assumed. The beam size at the focusing point is smaller than $\pm$ 2 cm for horizontal and

vertical directions.

3.2 Beam line spectrometer and counters

Both of the K^- in the beam and the π^- emitted after the reaction on the target should be momentum analyzed. At the K1.1 beam line, the last bending magnet (D4) together with Q10 and Q11 plays a role of the beam spectrometer. At the entrance of D4 we will install a tracking device (BFT) made of 1 mmϕ scintillating fibers arranged in 2 layers (0.5 mm pitch) and read by MPPCs. It has a time resolution less than 2 ns (FWHM), providing a powerful means to select a true track when multiple beam tracks are recorded. We successfully used the same detector for E10, E27 and E13 at K1.8. It has been confirmed at K1.8 that with this detector we can accept intense beam up to 3×10^7/spill(2 s) with a realistic bunched beam structure. The highest intensity of the 1.1 GeV/c K^- beam will be about 1.8×10^5 K^-/spill(2 s) for 50 kW operation with a comparable number of pion contamination, and the single count rate of the tracking detector at the upstream of D4 may be of the order of 10^6, which is much lower than the operation limit.

At the exit of the beam line, we install 1 mm-pitch MWPC's (BC3, BC4) which were used as BC1 and BC2 at the upstream of the beam line spectrometer at K1.8 for the E19 and E10 experiments.

We install plastic scintillator hodoscopes (BH1, BH2) with 5 mm thickness having a timing resolution of <150 ps (FWHM) each to separate K^- and π^- in the beam by time-of-flight. The same detectors were successfully used at K1.8 to completely separate kaons and pions at 1.8 GeV/c.[1]

The momentum resolution of the K1.1 beam line spectrometer is estimated to be 0.042% (FWHM) according to the simulation, which gives a negligible effect to the energy resolution of the hypernuclear mass spectrum with our thick targets ($\sim$20 g/cm^2).

The kaon beam is irradiated on a $^{nat}Li_2O$ (20 g/cm^2 for ^{7}Li) target. Just upstream and downstream of the target located are aerogel Cerenkov counters (BAC1,2 and SAC1) (see Fig. 15) to identify kaons in the beam and pions in the scattered particles.

3.3 SKS spectrometer

The scattered pions are identified and momentum-analyzed by use of the SKS magnet, tracking chambers (SDC1-SDC4), and TOF stop counters (TOF). The SKS magnet and the detectors are unchanged from the previous experiments at K1.8, but their geometrical setting will be changed from the E13 setting to the original one with a 100 degree bending angle of the central track. The SKS spectrometer sustains an acceptance of about 100 msr at maximum and covers a wide range of scattering angle ($|\theta| < 15^0$), we can populate non-spin-flip states at $|\theta| < 10^0$ and spin-flip states at $|\theta| > 10^0$ simultaneously, although the momentum acceptance becomes narrower than the E13 setting (that is not important in the proposing experiment at K1.1).

[1] In K1.1, the flight length between BH1 and BH2 is only 5 m, much shorter than the K1.8 case (11.1 m). However, the time-of-flight difference between 1.1 GeV/c K^- and π^- at K1.1 is 1.5 ns, which is still longer than the case of 1.8 GeV/c at K1.8 (1.3 ns).

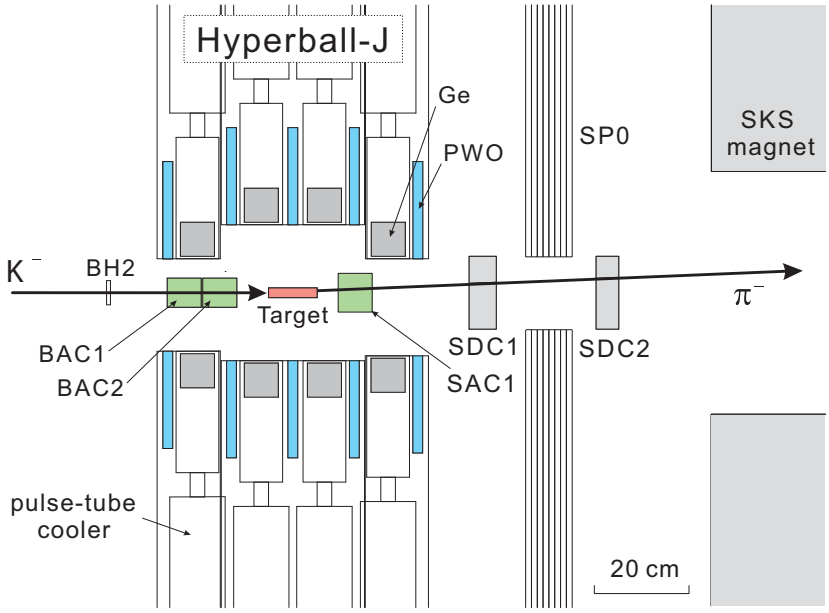

Figure 15: Experimental setup around the target and Hyperball-J (side view).

The SDC1,2 located upstream of the SKS magnet are 1 mm-pitch MWPC's, and SDC3,4 located downstream of the SKS magnet are large drift chambers with 2.5mm drift length. TOF is a plastic scintillator hodoscope wall with a 3 cm thickness for time-of-flight measurement between BH2 and TOF. In the previous experiments, pions and kaons were separated completely well at 1.0 GeV/c, our scattered π^- momentum for 1.1 GeV/c K^- beam. All the detectors have been successfully used at the K1.8 beam line for E19, E10, E27 and E13 without any serious trouble.

We expect to have a hypernuclear mass resolution better than 2.5 MeV (FWHM) without energy loss effect in the target. Thus, the actual mass resolution will be determined by energy loss effect in our thick (20 g/cm^2) target, which is estimated to be 6 MeV (FWHM), enough to tag the hypernuclear bound state region.

3.4 Background rejection counters

The beam K^- which decays in flight between BAC and SAC (namely, in the target region) as $K^- \to \mu^-\nu$ and $\pi^-\pi^0$ makes a serious background, not only in the trigger level but even after the full analysis of the hypernuclear mass, because μ^- and π^- from K^- decay enter the same kinematical region (momentum and scattering angle) as the π^- associated with hypernuclear production. In order to reject muons, we install a set of muon filters (SMF) made of a 50 cm-thick iron block and a hodoscope counter (LC) behind it. SMF successfully worked in E13 at K1.8. After adjusting the iron thickness, muons around 1.0 GeV/c, which causes serious background in the hypernuclear mass spectrum, will also be completely detected by LC and removed, and all the π^-'s associated with the hypernuclear production will not hit LC.

As for the $K^- \to \pi^-\pi^0$ decay modes, we detect π^0 by using 8 layers of lead-plastic sand-

wiched counters (SP0) which are installed between SDC1 and SDC2 and cover the forward angles except for the SKS entrance. In E13, by requiring hits in three or more layers of SP0, we detected high energy photons and rejected about 75% of the $K^- \to \pi^-\pi^0$ decay events which occurred in the target region (between BAC1,2 and ASC1). At $p_K^- = 1.1$ GeV/c, the rejection rate will be lowered to $\sim$ 60% The SP0 detectors successfully worked for E13 at K1.8.

3.5 Hyperball-J

The γ rays from hypernuclei are detected with Hyperball-J, a large germanium detector array dedicated to hypernuclear γ-ray spectroscopy at J-PARC. Hyperball-J was developed and constructed in 2011–2014 and successfully used for the E13 experiment at the K1.8 beam line in 2015. Figure 16 illustrates the lower half of Hyperball-J, and Fig. 17 shows photographs of Hyperball-J installed at K1.8.

Hyperball-J consists of 28 Ge detectors each of which has a Ge crystal of 60% efficiency relative to the ϕ 3"×3"NaI crystal. Each Ge crystal is mechanically cooled with a pulse-tube refrigerator [36], which decreases the crystal temperature down to 65–70 K, much lower than the temperature reached by liquid nitrogen (90–95 K), and greatly reduce serious effects of radiation damage peculiar to high-energy hadron beam experiments. This unique feature is particularly effective to reduce the systematic error due to radiation damage of Ge detectors for our $B(M1)$ measurement.

Each Ge detector is surrounded by PWO scintillation counters (20 mm thick) to suppress Compton scattering events, electromagnetic shower from high energy photons, and penetrating high energy particles. Compared to commonly-used BGO scintillator, PWO has a higher density and a larger effective atomic number, and emits a light with much shorter decay time ($\sim$ 10 ns). Although the light output of PWO is much smaller than BGO, we developed PWO counter having nearly 100% efficiency for 100 keV photons by using specially doped PWO crystal with a temperature lower than 0°C. The performance of the PWO background suppressor was confirmed in the E13 experiment as shown in Fig. 19. The background level decreased by a factor of $\sim$3 at 0.5–2 MeV.

Figure 18 shows the total photo-peak efficiency as a function of γ-ray energy for a point source and for the realistic condition considering the beam size and γ-ray absorption in the Li_2O target. In E13, the energy resolution for the final spectrum summed up for all the Ge detectors after energy calibration was 4.5 (FWHM) off the beam spill and 5.0 keV (FWHM) during the beam spill. Some of the Ge detector had worse resolution due to external electric noise from the power modules for the refrigerator. We are planning to change the power system to remove the noise.

In the E13 run at K1.8, these Ge detectors were confirmed to have an excellent performance at a high counting rate and a high energy deposit rate; under a typical condition for 5×10^5 $(K^-+\pi^-)$/spill(2.5 sec) and a 20 g/cm^2 CF_4 target [2] for a downstream Ge detector with the highest counting rate), the Ge detector live time during the beam spill was 80%. Therefore, the Ge detector live time in the proposing experiment is expected to be better than 80%

[2] In this condition, the Ge detector had a counting rate of 20 kHz and an energy deposit rate of 120 GeV/s.

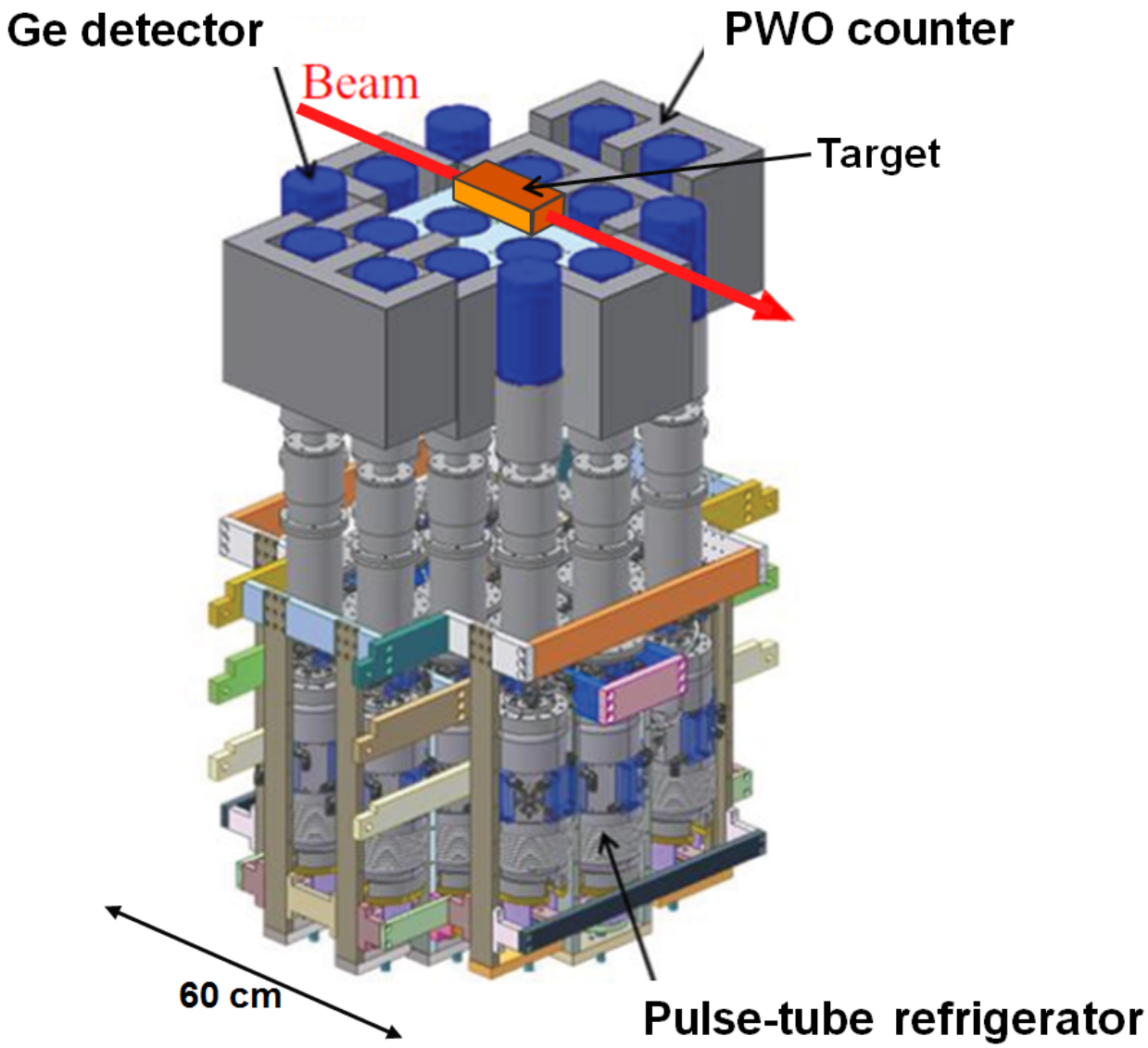

Figure 16: Schematic view of Hyperball-J (lower half only).

3.6 Trigger

In our CF_4 run in E13, the trigger was defined as

$$\mathrm{K_{in}} \times \mathrm{PI_{out}} \times \mathrm{Ge} = (\mathrm{BH2} \times \overline{\mathrm{BAC}}) \times (\mathrm{SAC} \times \overline{\mathrm{SP0}} \times \mathrm{TOF} \times \overline{\mathrm{SMF}}) \times (\Sigma_i \mathrm{Ge[i]}).$$

In the E13 run with 1.8 GeV/c beam of [3.6×10^5 K^- and 2.1×10^5 π^-]/spill, the trigger rate was 5.9×10^3/spill without SMF/SP0 and 2.1×10^3/spill with both SMF and SP0. Then we required a hit in more than one Ge detectors, then the trigger rate decreased to our acceptable value, 0.87×10^3/spill.

In the proposing experiment at K1.1, the beam rate (1.8×10^5 K^- and 1.3×10^5 π^- /spill) is lower by a half, but the $K^- \to \pi^-\pi^0$ decay rejection by SP0 is less effective (75% $\to$ $\sim$60

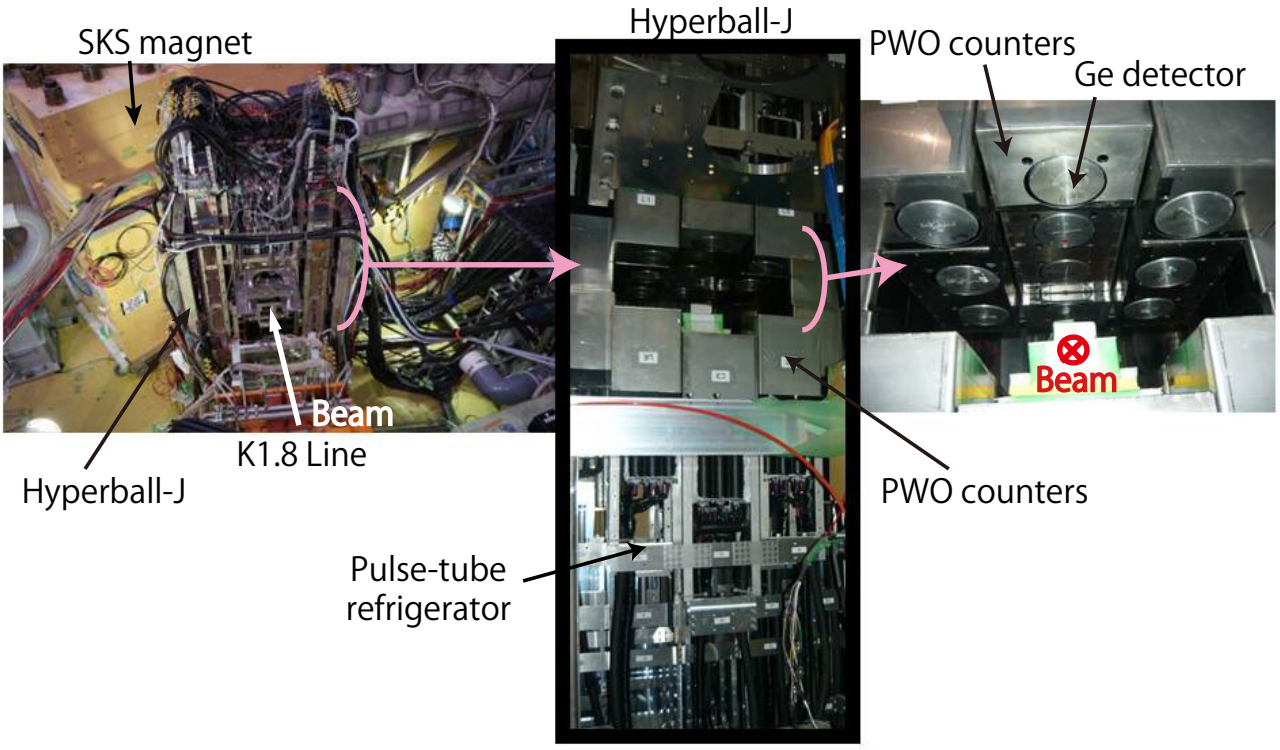

Figure 17: Photograph of Hyperball-J. Left: Hyperball-J installed in front of the SKS magnet. Center: Hyperball-J detectors with pulse-tube refrigerators viewed from upstream to downstream. Right: inner part of Hyperball-J.

%) due to lower beam momentum. In total, the trigger rate is estimated to be lower than 0.9×10^2/spill. In case the trigger rate is higher than 1×10^3/spill, we will include the PWO counters into the trigger. Using FPGA modules, we will make "valid γ trigger" by requiring that one or more Ge+PWO sets have a valid hit (Ge hit without ADC overflow and no PWO hit in any of the surrounding PWO counters). It will greatly reduce the trigger rate to be less than 0.5×10^2/spill.

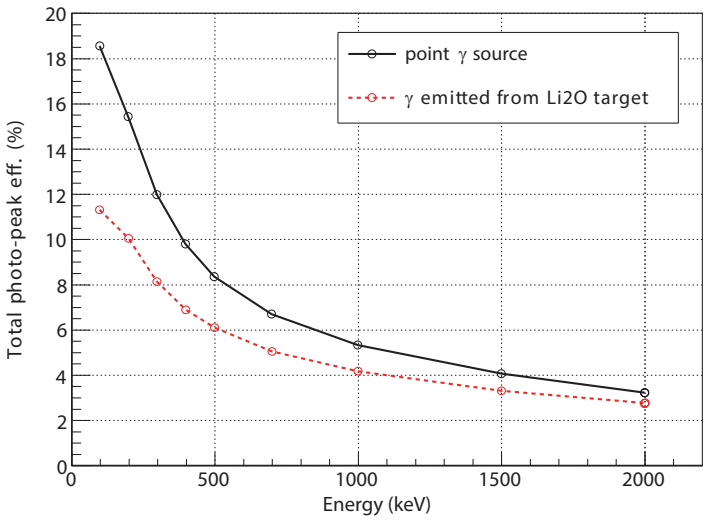

Figure 18: Simulated efficiency curve of Hyperball-J (with 28 Ge detectors) for a point source and for realistic conditions with a source point distribution and absorption in the Li_2O target taken into account.

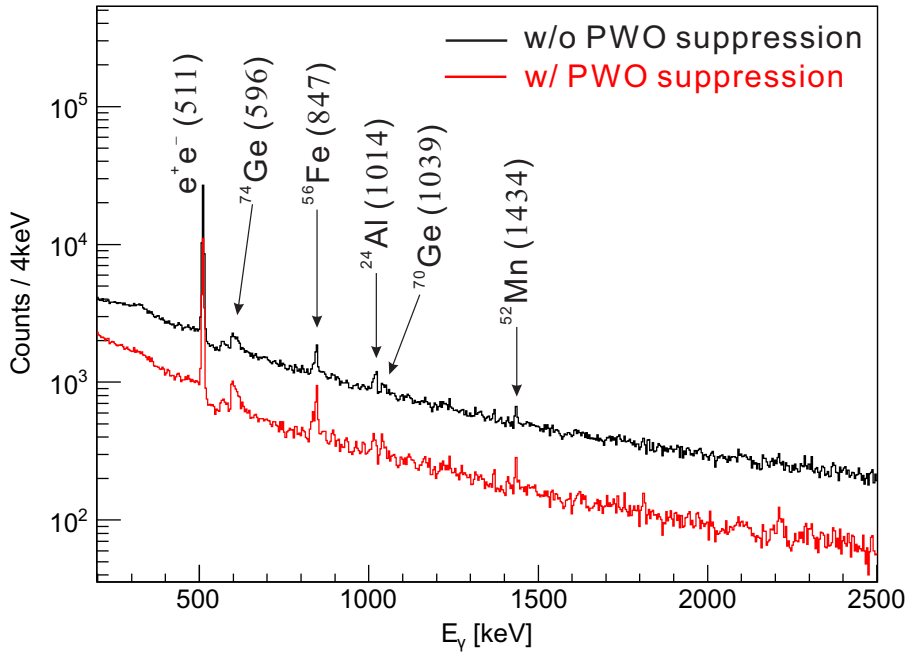

Figure 19: Performance of the PWO counters. Shown are the γ-ray spectra measured by Hyperball-J without event selection in the E13 beam time, (black) without and (read) with background suppression using PWO counters.

4 Beam time request and schedule

4.1 Experiment (1) : Yield estimate

The production cross section of the ${}^{4}_{\Lambda}\mathrm{H}(1^{+})$ state in the in-flight ${}^{7}\mathrm{Li}(K^{-},\pi^{-})$ reaction is unknown, but the BNL experiment [31] provides a rough estimate of the yield. In the BNL experiment, 1×10^{10} K^{-}'s (0.83 GeV/c) were bombarded on a 8 g-thick lithium target and γ-rays were detected with NaI counters having a 6% photo-peak efficiency at 2 MeV. The data were taken at very forward angles ($\sim 0^{\circ}$) in the (K^{-},π^{-}) reaction, where the π^{-} spectrometer acceptance, not given in literatures, is supposed to be 18 msr or less. They observed 50±29 counts of the 1.1 MeV γ ray with the S/N ratio ~ 1 at the peak center.

Table 1 shows the expected yield roughly estimated by comparing with the BNL experiment. If we assume that ${}^{4}_{\Lambda}\mathrm{H}$ production occurs via the substitutional $(s)_{n}^{-1}(s)_{\Lambda}$ state ($E_{ex} \sim 20$ MeV) and is thus dominated at forward angles ($< 6^{\circ}$), a part of our large SKS acceptance (∼100 msr) is effective. The efficiency of Hyperball-J can be increased by arranging each Ge detectors closer to the target, since the Doppler shift correction is not important as shown in Fig. 10 and the counting rate of our Ge detectors is expected to be much lower than the operation limit. The DAQ and analysis efficiencies are assumed to be the same. In 5 days' beam time, we expect to collect ∼300 events or more for the ${}^{4}_{\Lambda}\mathrm{H}$ γ rays. As described in Sect. 2.1, the ${}^{4}_{\Lambda}\mathrm{H}$ γ-ray peak suffers from Doppler broadening due to fragmentation, which cannot be corrected for. In the BNL experiment, the Doppler broadening did not matter due to NaI counter resolution (90 keV (FWHM) at 1.1 MeV), but in our experiment with Ge detectors, the peak width can be narrower, particularly by selecting the mass region close to the threshold (E_{ex} = 20–25 MeV), as shown in Fig. 10 (b). Here, the expected width is $\sigma \sim 18$ keV, and the peak counts may be $\sim$ 1/4 of the BNL case (E_{ex} = 22–39 MeV), 75 counts. The error of the peak center position will be $\sigma \sim 18/\sqrt{75} = 2.1$ keV without background, and the effect of the background is expected to be much smaller. Therefore, we expect to determine the ${}^{4}_{\Lambda}\mathrm{H}$ γ-ray energy in a statistical error of ±3 keV Since the systematic error will be comparable or smaller, and the total accuracy less than 5 keV will be achieved.

Thus we request 5×10^{9} K^{-} on target, which corresponds to a beam time for 6 days in 50 kW - 6s cycle operation.

Table 1: Yield estimate of the proposing ${}^{4}_{\Lambda}\mathrm{H}$ γ-ray measurement in comparison with the BNL experiment [31].

	BNL exp.	Proposing exp.
Number of K^{-}	1×10^{10}	0.5×10^{10} (6 days)
Target	8 g/cm^2 for ^{nat}Li	15 g/cm^2 for ^{7}Li
γ-ray efficiency (at 2 MeV)	6%	3%→6%
Effective π^{-} acceptance	<18 msr?	∼35 msr ($< 6^{\circ}$)
${}^{4}_{\Lambda}\mathrm{H}$ γ-ray counts	150	>300

Table 2: Expected yield in the ${}^{7}_{\Lambda}$Li experiment for K^- momenta of 0.9 and 1.1 GeV/c. Cross sections are scaled from calculated ones for 1.5 GeV/c (Fig. 11).

Hypernucleus	${}^{7}_{\Lambda}$Li			
State produced by (K^-,π^-)	$1/2^+(T{=}1)$	$3/2^+$	$1/2^+(T{=}1)$	$3/2^+$
it excitation energy (keV)	3877	692	3877	692
p_{K^-} (GeV/c)	0.9		1.1	
$d\sigma/d\Omega$ @5°(μb/sr)	84	0	19	1.6
$d\sigma/d\Omega$ @10°(μb/sr)	120	0	22	8.8
$\int_{2^\circ}^{20^\circ} d\sigma/d\Omega \cdot \delta\Omega$ (μb)	13	0	2.0	0.74
Target[^{7}Li in Li_2O(10 cm^t, ρ =2.01g/cm^3)]	0.87 g/cm^3×10 cm×6.02×10^{23}/7 = 7.48×10^{23} /cm^2			
N_{K^-} /spill (×10^3)	56		176	
N_{K^-} /hour	×600 spill/hour			
detector/analysis efficiency	0.6			
Yield/hour/μb	15.1		47.4	
${}^{7}_{\Lambda}$Li mass peak counts /hour	196	0	95	35
Cascade Transition	$\rightarrow 3/2^+$	$\rightarrow 1/2^+$	$\rightarrow 3/2^+$	$\rightarrow 1/2^+$
Branching ratio of $1/2^+(T{=}1)\rightarrow 3/2^+$	0.25*	1	0.25*	1
γ peak efficiency at 692 keV	0.051			
Ge live time	0.8			
γ counts /hour	2.0	0	0.97	1.43
γ counts /hour (total)	2.0		2.4	

* Experimental result from KEK E419

4.2 Experiment (2) : Yield estimate

Table 2 shows the yield estimate of the ${}^{7}_{\Lambda}$Li($3/2^+\rightarrow 1/2^+$) γ ray at 692 keV. As for the cross sections of the ${}^{7}_{\Lambda}$Li states, we used DWIA calculations for $p_{K^-} = 1.5$ GeV/c by Motoba (Fig. 11) and scaled for $p_{K^-} = 1.1$ and 0.9 GeV/c considering difference of momentum transfer and the spin-flip/non-flip elementary cross sections in Fig. 9. As for the K^- beam intensity, we assumed 1.76×10^5 per spill for 1.1 GeV/c and 0.56×10^5 per spill for 0.9 GeV/c, which are expected for 50 kW proton beam power according to a simulation using Decay Turtle code. The realistic photo-peak efficiency of Hyperball-J array for the Li_2O target shown in Fig. 18 (0.051 at 692 keV), as well as the Ge detrector live time (80%) measured in E13 with a beam intensity of 4×10^5 (K^-+π^-)/spill is used. The yield of the $3/2^+ \rightarrow 1/2^+$ γ ray is estimated to be comparable between 1.1 and 0.9 GeV/c.

Figure 20 shows simulated spectra of the γ ray for K^- momentum of 0.9 GeV/c and 1.1 GeV/c. Here we assumed the beam time of 35 days to collect about 2000 events of the transition. The γ-ray background level was estimated from the ${}^{7}_{\Lambda}$Li γ-ray spectrum, Fig. 5 (a), and the background contribution from ^{16}O estimated from Fig. 12 was added. It should be noted that the background level also depends on (1) the Ge detector timing cut width determined by the Ge timing resolution and (2) PWO(BGO) background suppression factor. But these effects are

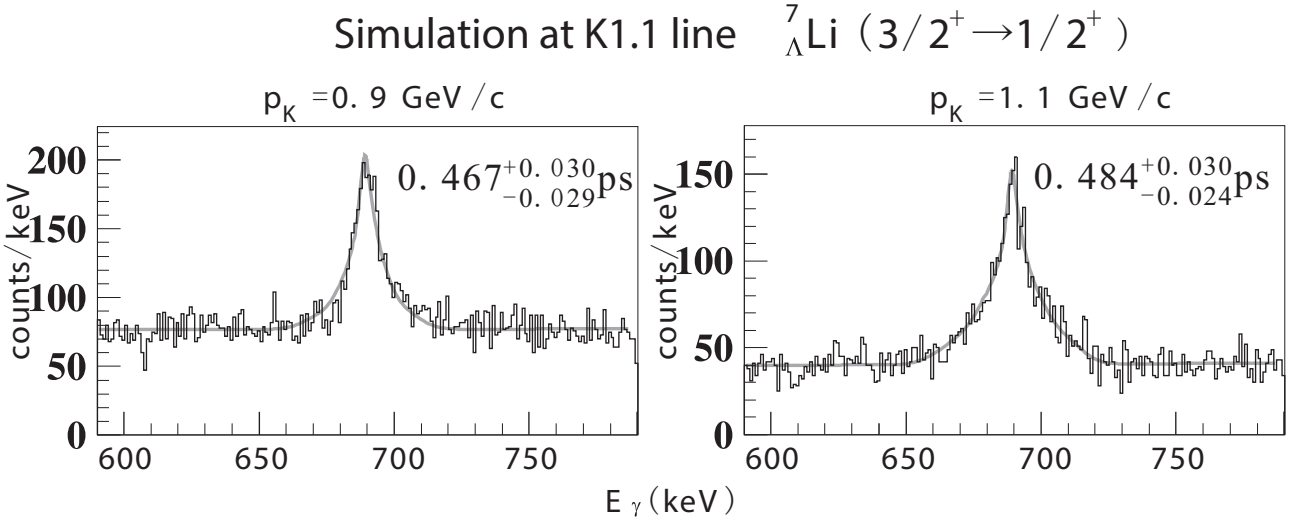

Figure 20: Simulated γ-ray spectrum of the ${}^{7}_{\Lambda}$Li($3/2^{+}\rightarrow 1/2^{+}$) transition for K^- momentum of 0.9 GeV/c and 1.1 GeV/c at the K1.1 beam line. A beam time of 35 days with 50 kW (gold target) is assumed. The peak is fitted with calculated peak shapes for various lifetimes and the accuracy of the lifetime was found to be 6%.

expected to be similar.[3]

For each beam momentum, the simulated peak was fitted with the peak shapes calculated for various lifetimes. The obtained lifetime is given in the figure. The error for the lifetime ($\sim$6%) is almost the same between 1.1 and 0.9 GeV/c. Thus, the $B(M1)$ value will be obtained in a statistical error of 6%, and consequently the $|g_\Lambda - g_c|$ value in 3%, with a systematic error smaller than the statistical error as discussed in Sect. 2.2.4.

In the case of 1.1 GeV/c, the S/N ratio is better than the 0.9 GeV/c case due to a large cross section of the direct spin-flip production of $3/2^{+}$ state but less cross sections for the background process coming from the non-spin-flip ${}^{7}_{\Lambda}$Li $1/2^{+}$ and $5/2^{+}$ states as well as the ${}^{16}_{\Lambda}$O states. However, the accuracy of the lifetime determination is similar because the slower recoil velocity in the 0.9 GeV/c case has better sensitivity in DSAM. It is not clear which momentum is better in the present simulation. Since there are ambiguities in the K^- beam intensity, the ${}^{7}_{\Lambda}$Li cross sections, the background levels, etc., test runs with both beam momenta is desired to optimize the experimental condition.

4.3 Beam request including commissioning/control runs

The commissioning and control runs as well as the production runs are listed below. We request to run in two periods which are separated by more than 4 months.

[3](1) In E419, the Ge timing cut width at 692 keV was 80 ns, and about 15% of the events at 692 keV were accidental background [37]. It will be much reduced by our timing cut width of $\sim$ 20 ns. (2) In E419, the BGO suppression factor was 3.0 [37], while the PWO suppression factor at 692 keV in E13 was 2.6 due to imperfect coverage by PWO. It makes the background level 15% higher.

The 1st period:

- Detector tuning (Spectrometers/Hyperball-J) : 5 days
- Beam tuning for 1.1 GeV/c and 0.9 GeV/c: 5 days
- 1.1 GeV/c control runs (beam-through, minimum bias trigger, etc.): 0.5 day
- 0.9 GeV/c control runs (beam-through, minimum bias trigger, etc.): 0.5 day
- 1.1 GeV/c ^{12}C (spectrometer resolution test and missing mass calibration): 0.5 day
- 0.9 GeV/c ^{12}C (spectrometer resolution test and missing mass calibration): 0.5 day
- 0.9 GeV/c ^{7}Li ($^{4}_{\Lambda}$H production run): 6 days
- 1.1 GeV/c Li_2O ($B(M1)$ sensitivity test): 2 days
- 0.9 GeV/c Li_2O ($B(M1)$ sensitivity test): 2 days

The 2nd period:

- 1.1 GeV/c or 0.9 GeV/c Li(thin) (Mass spectrum of $^{7}_{\Lambda}$Li): 2 days
- 1.1 GeV/c or 0.9 GeV/c ^{16}O (H_2O) (Background from ^{16}O): 1 days
- 1.1 GeV/c or 0.9 GeV/c Li_2O ($B(M1)$ production run): 35 days

Since this will be the first experiment using the K1.1/SKS spectrometers, detector tuning and beam line tuning will take a significant time. The requested time (5+5 days) is estimated from our experience of starting-up the K1.8 beam line.

After control runs and magnetic spectrometer test/calibration runs with a thin ^{12}C target for two days in total, the production run for $^{4}_{\Lambda}$H (0.9 GeV/c, thick ^{7}Li target) for 6 days will be carried out. Then, we will take test data for a Li_2O target with 1.1 GeV/c and 0.9 GeV/c K^- beam momenta to measure the yield and the S/N ratio to see which of them has better sensitivity for $B(M1)$ measurement. After analyzing these test data, the beam momentum and the total beam time for $B(M1)$ will be finally decided.

In the 2nd period, by using the K^- beam momentum decided as 1.1 or 0.9 GeV/c, we will carry out a production run for 35 days for the $B(M1)$ measurement, together with control runs with a thin Li target to measure the $^{7}_{\Lambda}$Li mass spectrum, as well as with a thick H_2O target to measure the background contribution in the Li_2O target run.

In these runs, we suppose the accelerator operation of 50 kW proton beam power and 6 s cycle, assuming the K^- intensity of 1.76×10^5 per spill for 1.1 GeV/c and 0.56×10^5 per spill for 0.9 GeV/c. The beam time length depends on the available K^- intensity.

4.4 Readiness

The upstream part of the K1.1 beam line (K1.1BR) has been used for many test experiments and E36, while the downstream part of K1.1 should be assembled. The SKS magnet is just being moved from the K1.8 area to the K1.1 area, of which work will be finished by the end of March in 2016.

Most of the detectors (BH2, BC3, BC4, SDC1, SDC2, SDC3, SDC4, SP0, TOF, SMF) are ready; they were used at K1.8 and will be moved to K1.1. We need to fabricate or modify beam line trigger counters (BH1, BFT, BAC1-2 and SAC1-2), of which cost and manpower are small. We are also planning to repair broken wires in SDC3 and SDC4, which will take a half year but almost no cost.

As for Hyperball-J, we need maintenance (evacuate, and anneal if necessary, all the Ge detectors) just before the beam time and mount them to the Hyperball-J frame, which will take 3 months with no cost.

The total cost including additional electronics and HV modules will be less than 20M yen, which is covered mainly by the spokesperson's Grant-in-Aid. We also plan to replace the TDC modules for the drift chambers from the old TKO system into faster new modules to reduce the DAQ dead time, but it depends on development status of new TDC modules and our budget.

4.5 Schedule

We can start installation of all the detectors for the beam/SKS spectrometers just after the K1.1 beam line construction is finished. The detector installation will take 4 months.

The power modules for the Ge detector refrigerators in Hyperball-J will be upgraded in 2016 so as to reduce noise from power lines and improve the energy resolution. Then Hyperball-J will be used for E03 experiment (Ξ-atomic X-rays) at K1.8 [38], which will most probably run in 2016-2017. After E03, we need to perform maintenance and then install all the detectors of Hyperball-J at K1.1. So we hope to run at least 3 months after E03 is finished.

References

[1] D.H. Davis, Nucl. Phys. A 754 (2005) 3c.

[2] A. Nogga, H. Kamaza, W. Gloeckle, Phys. Rev. Lett. 88 (2002) 172501.

[3] A. Esser *et al.*, Phys. Rev. Lett. 114, 232501 (2015).

[4] T.O. Yamamoto *et al.*, Phys. Rev. Lett. 115 (2015) 222501.

[5] M. Bedjidian *et al.*, Phys. Lett. B 83, 252 (1979).

[6] M. Bedjidian *et al.*, Phys. Lett. B 62, 467 (1976).

[7] A. Kawachi, Docter thesis, University of Tokyo, 1997.

[8] A. Gal, Phys. Lett. B 744 (2015) 352.

[9] D. Gazda and A. Gal, arXiv:1512.01049[nucl-th].

[10] E. Hiyama, M. Kamimura, T. Motoba, T. Yamada and Y. Yamamoto, Phys. Rev. C 65 (2002) 011301(R).

[11] H. Nemura, Y. Akaishi and Y. Suzuki, Phys. Rev. Lett. 89 (2002) 142504.

[12] E.V. Hungerford and L.C. Biedenharn, Phys. Lett. B 142 (1984) 232; T. Yamazaki, Nucl. Phys. A 446 (1985) 467c.

[13] T. Takeuchi, K. Shimizu, K. Yazaki, Nucl. Phys. A 481 (1988) 693.

[14] R.H. Dalitz and A. Gal, Ann. Phys. **116** (1978) 167; J. Phys. G 6 (1978) 889.

[15] C.B. Dover, H. Feshbacj and A. Gal, Phys. Rev. C51 (1995) 541.

[16] K. Saito, M. Oka, T. Suzuki, Nucl. Phys. A 625 (1997) 95;
M. Oka, K. Saito, K. Sasaki, T. Inoue, *"Hadrons and Nuclei"* ed. Il-T. Cheon *et al.*, American Institute of Physics (2001) p.163.

[17] H. Tamura *et al.*, Phys. Rev. Lett. 84, 5963 (2000).

[18] K. Tanida *et al.*, Phys. Rev. Lett. 86, 1982 (2001).

[19] Y. Miura *et al.*, Nucl. Phys. A 754 (2005) 75c.

[20] Y. Ma *et al.*, Nucl. Phys. A 835 (2010) 422.

[21] K. Hosomi *at al.*, Prog, Theor. Exp. Phys. 2015 (2015) 8, 081D01.

[22] M. Ukai *et al.*, Phys. Rev. C 73 (2006) 012501.

[23] E. Hiyama, M. Kamimura, K. Miyazaki and T. Motoba, Phys. Rev. C 59 (1999) 2351.

[24] H. Akikawa *et al*, Phys. Rev. Lett. 88, 082501 (2002).

[25] M. Ukai *et al.*, Phys. Rev. Lett. 93 (2004) 232501.

[26] H. Tamura *et al.*, Nucl. Phys. A 754 (2005) 58c.

[27] T. Motoba, H. Bandō and K. Ikeda, Prog. Theor. Phys. **80** (1983) 189.

[28] H. Tamura et al., J-PARC proposal E13, "Gamma-ray spectroscopy of light Λ hypernuclei".

[29] H. Tamura, M. Ukai, T.O. Yamamoto, and T. Koike, Nucl. Phys. A 881 (2012) 310.

[30] T. Takahashi *et al.*, Prog. Theor. Exp. Phys. (2012) 02B010.

[31] M. May *et al.*, Phys. Rev. Lett. 51 (1983) 2085.

[32] G.P. Gopal *et al.*, Nucl. Phys. B 119 (1977) 362.

[33] T. Harada, Private communication (2006).

[34] T. Motoba, private communication (2006).

[35] J.F. Ziegler *et al.*, "SRIM–The Stopping and Range of Ions in Matter", *http://www.srim.org/*

[36] T. Koike *et al.*, Nucl. Instr. Meth. A 770 (2014) 1.

[37] K. Tanida, Docter thesis, University of Tokyo, 2000.

[38] K. Tanida *et al.*, J-PARC proposal E03, "Measurement of X rays from Ξ^- Atom".